

# Chapter 1

## Frictional Force—Introduction

**Abstract** This first chapter begins with an introduction to BFMC, covering basic systemic definitions and nature of friction material composites applied to automotive braking systems. The rudimentary aspects of friction material composite with their definitions based on polymeric, metallic, and multiple matrix with some of the issues at the interphases are discussed to give an account of the fundamentals. AFM (Atomic Force Microscopy), FIM (Field Ion Microscope), and MD (Molecular Dynamics) observations, a study of size of the asperity in situ and a transition from “Microscopic Single Atom” friction to “Macroscopic” friction are also discussed. Independence of the coefficient of friction from weight and velocity, based on the governing factors of frictional force and molecular forces, are explained. An account of what exactly happens in a frictional contact surface as a heat affected film or layer is explained in this chapter. Relationships between the aperiodic atomic structure of quasicrystals and their effect on lowering friction, for both elastic and inelastic regimes, are brought to the limelight with their effect on crystallographic planes of contact. The significance of quasicrystals, in the future research, applied to brake friction material composites and their usefulness are explained in brief. Essential virtues of BFMC with its theoretical considerations of static, kinetic-coefficiency are highlighted. Further, hot and cold compressibility measurements in BFMC, low- and high-speed judder characteristics and its relation to noise, and its role in static and dynamic coefficiency are explained. Basic information on the science of noise as applied to braking contact and its possible elimination sequence with matrix alteration will find a useful input in the introductory chapter.

### 1.1 Introduction

This introductory book on brake friction material composite covers areas of basic friction, contact (rigid) rotor or a drum, and contacting (relatively flexible) disk pad, liner, or composition brake block surfaces and how the surfaces relatively work while braking in automobile, rail, and similar braking applications.

This volume is designed to give introductory aspects to a wider audience that wishes to know more about basic definitions of friction material composite applied to braking, frictional force and how functionally raw materials work on integration into the friction material composite system. Basic design of friction, wear and other related issues like judder, noise, DTV (disk thickness variation), RTV, (rotor thickness variation), etc., while braking have been discussed.

## 1.2 BFMC—Brake Friction Material Composite—Definition

Brake friction material composite system could be brought under the definition of a nonlinear, multimatrix, multicomponent, dynamic, aperiodic, deterministic system—partially random.

### 1.2.1 Characteristics Defining the System

*Nonlinear*—Seemingly unpredictable behavior which will respond disproportionately (nonlinearly) to initial conditions.

*Deterministic*—Quantifiably predictable pattern of values on measurements made. Nonlinear interaction of few variables—mutually interdependent as opposed to a large number of variables, which is defined as stochastic. Both are typically classified under randomness.

*Partially random*—Some of the properties are determinable even before the experiment is conducted. A random experimental measurement is possible with a numeric quantity of a random variable.

While explaining quantity of a random variable in BFMC, probability density function could be defined and explained; say  $f(x)$  equals 1 calculated over a range of  $x$ .

If  $f(x)$  is a probability density function of a continuous random variable,  $x$  can assume values between  $x = a$  and  $x = b$ , then

$$\int_a^b f(x) dx = 1$$

It is possible that the forms of a probability density function could vary anywhere in the range for which it is defined through random experimental measurement. Probability density function could be explained as below:

It can take any number of forms

$$f(x) = 4 \times 3 \quad \text{for} \quad 0 \geq x \leq 1$$

where  $f(x)$  is positive for all real values of  $x$  (Fig. 1.1).

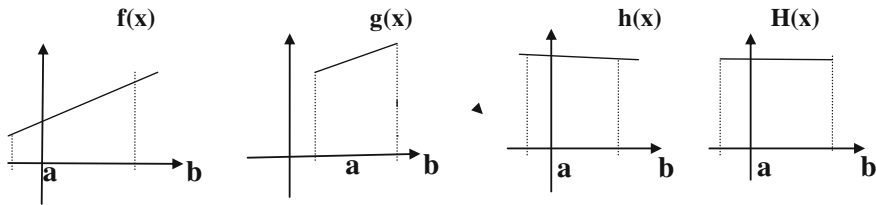


**Fig. 1.1** Several forms of probability density functions

$$\int_0^1 f(x) dx = \int_0^1 4x^3 dx = 4(x^4/4) \int_0^1 1$$

With a probability density function  $f(x) = 4x(1 - x^2)$  for  $0 \leq x \leq 1$ .

Similarly, we can determine the probability that the random variable of any material constituent in BFMC system can fall between 0.2 and 0.4 or any other range in contemplation while designing the materials (Fig. 1.2).

$$\begin{aligned} \int_{0.2}^{0.4} 4x(1 - x^2) dx &= \int_{0.2}^{0.4} 4(x^2/2 - x^4/4) \\ &= 4\{(0.16/2 - 0.0256/4) - (0.04/2 - 0.0016/4)\} \\ &= 0.216 \end{aligned}$$

The sought probability is 0.216 in this case, corresponding to the shaded area of the graph in Fig. 1.2.

A mathematical design model for multiple random variables in BFMC with varying quantities of materials as random variables could be applied to get the probable range of constituents, which could be integrated into the system.

*Dynamic*—Continuous changes leading to minor physical and frictional alteration with single independent variable time.

*Aperiodic*—Time variant on application (like the variance in air which is in the medium of sound and is not the medium of sound).

When we say aperiodic time variant in a friction material context, time could never be constant if we consider the speed of light or sound as constant. In a unidimensional spacetime, time is measured as the relative velocity of the reference with which it is measured. When we travel through time we always travel through time only, when we travel through space, we travel through time by less than what is expected. Time in a moving system for an observer who is stationary observes it to be running slower by a factor of “ $t$ ”.

When we talk about spacetime, time and space are relative but the geometry of space is different. Gravitational effects in terms of geometry can explain hyper-space, rather than the attracting and repelling forces. Hence gravitational mass and

**Fig. 1.2** Probability density graph

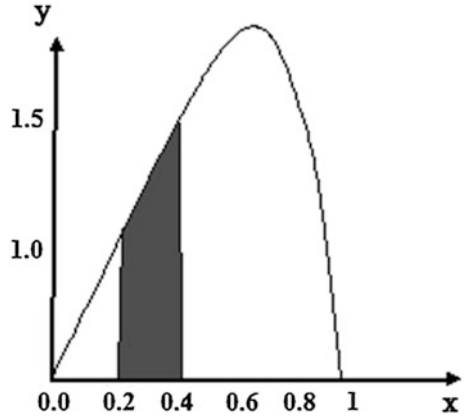
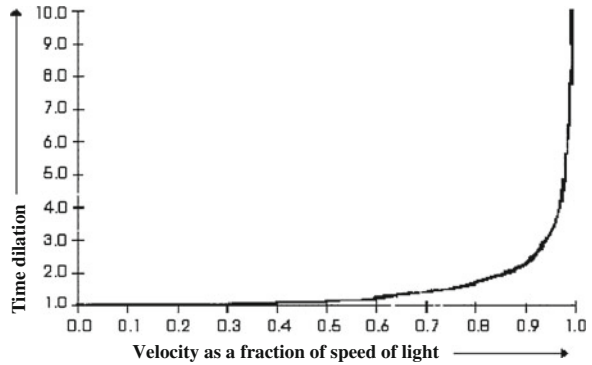


**Fig. 1.3** Time dilation against velocity



inertial mass could be equated which also explains the principle of equivalence, which could be applied to braking principle.

*The effect of time dilation appears negligible with the speed of a car or train or a plane but it increases exponentially when you travel close to the speed of light (Fig. 1.3). Nearer to the speed of light “c”, time virtually stands still for the observer.*

Velocity expressed as a fraction of the speed of light versus time dilation is plotted on a scale and is expressed as  $t' = t / \sqrt{1 - v^2/c^2}$ .

### 1.2.2 Nature of Brake Friction Material Composite (BFMC)

*Multicomponent*—Multiple or  $N$  mutually interacting point mass objects which move in three dimensions.

Consider a system of  $N$  mutually interacting point mass objects which move in three dimensions (Fig. 1.4). Let the  $i$ th object, whose mass is  $m_{ij}$ , be located at vector

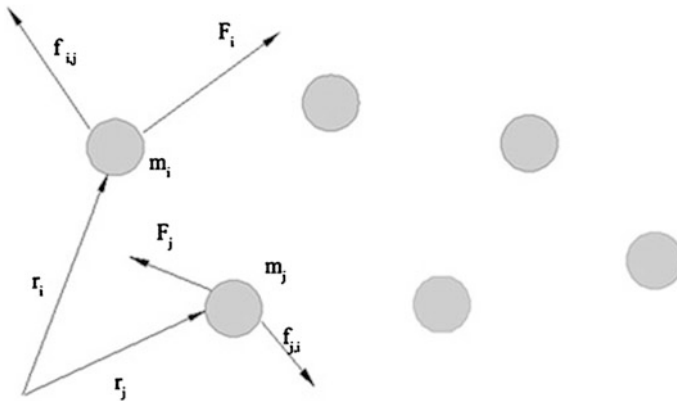


**Fig. 1.4** Three-dimensional dynamic system with multiple mass objects

displacement  $r_{ji}$ . Suppose this object exerts a force  $F_{ji}$  on the  $j$ th object. By Newton's third law of motion, the force  $f_{ij}$  exerted by the  $j$ th object on the  $i$ th is given by

$$f_{ij} = -f_{ji}$$

Suppose that the  $i$ th object is subject to an external force  $F_i$ , Newton's second law of motion applied on the  $i$ th object yields

$$j \neq i \quad m_i r_i = \sum f_{ij} + F_i, \quad j = I, N$$

Summation of the right-hand side of the equation excludes the case  $j = i$ , since  $i$ th object cannot exert a force on itself, we sum it over all objects

$$j \neq i, \quad \sum m_i r_i = \sum f_{ij} + \sum F_i \quad I = 1, N \quad I, j = I, N \quad I = I, N$$

*Multimatrix*—It is an integrated matrix material that surrounds and supports the reinforcement materials by maintaining their relative positions. It could be metallic, polymeric, etc.

*Heterogeneous*—Not uniform in nature, formed of parts or elements that are all not of the same kind.

Brake friction material composite—is heterogeneous at least to a certain minimum degree and could never be classified as homogeneous.

#### **a. Atomic Packing Factor**

Volume of atoms/Volume of unit cell

$$(4/3)\pi r^3 / a^3 = (4/3)\pi r^3 / (2r^3) = 0.52$$

Body centered  $a = 4r/\sqrt{3}$

$$\frac{4}{3} \pi r^3 / a^3$$

$$\frac{4}{3} \pi r^3 / \left(4r/\sqrt{3}\right)^3 = 0.68$$

Face centered  $a = 4r/\sqrt{2} = 0.74$

## b. Significance of Atomic Packing Models

With the atomic packing factor, models that illustrate packing can serve completely different purposes in the case of a nuclear crystal model. Atomic packing models can help in the study and understanding of gliding, coordination, exsolution, isomorphism, polymorphism, cleavage, and the innate relationship between crystal structure and their habits. It also helps us understand issues related to atomic positions, their relative sizes, and atomic packing factor. In the case of nuclear models, they are restricted to show the symmetry and point positions, whereas relative atomic radii could be more understood in atomic packing models.

For instance, in a zircon crystal structure with the unit cell dimension  $a = 6.58$  Å and  $c = 5.93$  Å.

Zr is equipoint  $b$  symmetry Vd at  $[0, 0, 0]$ .

Si is equipoint  $a$  symmetry Vd at  $[0, 0, \frac{1}{2}]$ .

O is equipoint  $h$  reflection planes at  $[o, u, v]$  where it is 0.20 or one-fifth the unit cell dimension  $a$ , and  $v = 0.34$  or one-third  $c$ .

The Si atom coordinates  $[0, 0, \frac{1}{2}]$  have the following:

Neighbors	Coordinates	Distance
4O	$0, u, \frac{1}{2} - v$	1.62 Å
2Zr	$0, 0, \frac{1}{2}$	2.97 Å
8O	$\frac{1}{2}, u, v - \frac{1}{4}$	3.58 Å
A Zr coordinates $[0, 0, 0]$ has		
4O	$0, \frac{1}{2} - u, \frac{1}{4} - v$	2.05 Å
4O	$0, u, v$	2.41 Å
2Si	$0, 0, \frac{1}{2}$	2.97 Å

Structure is made of strings parallel to the  $c$  axis with alternate  $\text{SiO}_4$  and Zr units. Each Zr atom joins the  $\text{SiO}_4$  tetrahedra from the four neighboring strings. The shortest distance between the Zr and O atom is the sum of their radii as they touch each other. From these, atomic radii of O is 1.32 Å and Zr = 0.73 Å. From these  $\text{SiO}_4$  tetrahedra models with bridges of two tetrahedra and one zirconium atom, bridges could be modeled (Fig. 1.5).

With this, packing model of zircon and oxygen, which could be built with spherical balls with their drilling coordinates, could be built depending on the

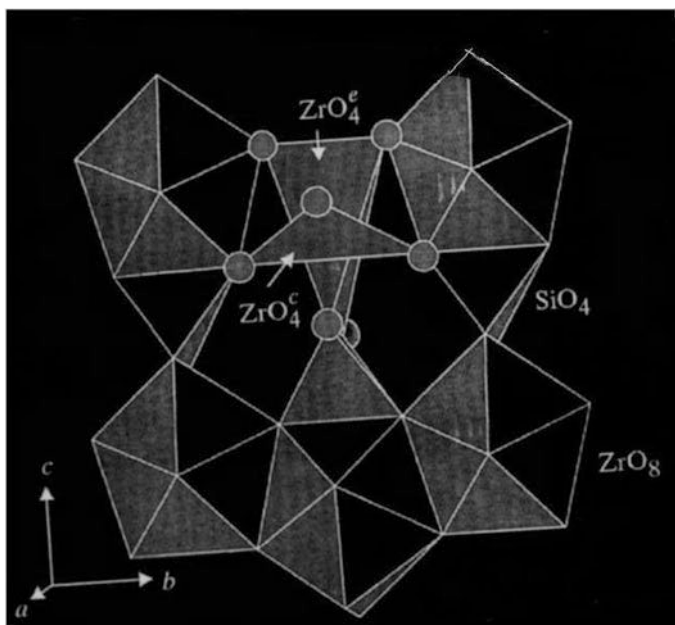


**Fig. 1.5** Zirconium silicate crystalline structure

scaling of the ball diameter  $O$ , the drilling coordinates with the number of spherical balls required for one or two unit cells.

When atoms are in motion, lattice vibrations are induced in the substrate when the energy or heat flows away from the interface.

When two surfaces slide past each other, simulations enhance our understanding of the processes that occur. Good knowledge of the mechanisms acts as a clear basis on the setup to bring up an effective interpretation of the simulation. Realistic surface profiles of the rotor contact with the BFMC and the detailed test conditions like pressure distribution, shear contact, and temperature profile needs can present a better understanding of what could be the scope of the simulation. Issues pertaining to nanoscale systems throw light on the lube performance vis a vis frictional changes and how the wear is induced.

Compacted oxide layer glaze describes the often shiny, wear-protective layer of oxide formed when two metals (or a metal and ceramic) are slid against each other at high temperature in an oxygen-containing atmosphere. The layer forms on either or both the surfaces in contact and can protect against wear.

A not often used definition of *glaze* is the highly sintered compacted oxide layer formed due to the sliding of either two metallic surfaces or sometimes a metal surface and ceramic surface at very high temperatures (normally several hundred degrees celsius) in oxidizing conditions. The sliding or tribological action generates oxide debris that can be compacted against one or both sliding surfaces and, under the correct conditions of load, sliding speed, and oxide chemistry as well as (high)

temperature, sinter together to form a “glaze” layer. The “glaze” formed in such cases is actually a crystalline oxide, with a very small crystal or grain size having been shown to approach nanoscale levels. Such “glaze” layers were originally thought to be amorphous oxides of the same form as ceramic glazes, hence the name “glaze” is currently used.

Such “glazes” have attracted limited attention due to their ability to protect the metallic surfaces on which they may form, from wear under the high temperature conditions in which they are generated. This high temperature wear protection allows potential use at temperatures beyond the range of conventional hydrocarbon-based, silicone-based, or even solid lubricants such as molybdenum disulfide (the latter useful up to about 450 °C short term). Once they form, little further damage occurs unless there is a dramatic change in sliding conditions.

Such “glazes” work by providing a mechanically resistant layer, which prevents direct contact between the two sliding surfaces. For example, when two metals slide against each other, there can be a high degree of adhesion between the surfaces. The adhesion may be sufficient to result in metallic transfer from one surface to the other (or removal and ejection of such material)—effectively adhesive wear (also referred to as *severe wear*). With the “glaze” layer present, such severe adhesive interactions cannot occur and wear may be greatly reduced. The continued generation of oxidized debris during the more gradual wear that results (entitled *mild wear*) can sustain the “glaze” layer and maintain this low wear regime.

However, their potential application has been hampered as they have been only successfully formed under the very sliding conditions where they are meant to offer protection. A limited amount of sliding damage (referred to as “run in wear”—actually a brief period of adhesive or severe wear) needs to occur before the oxides are generated and such “glaze” layers can form. Efforts at encouraging their early formation have met with limited success and the damage inflicted during the “run in” period is one factor preventing this technique from being used in practical applications.

As oxide generated is effectively the result of the tribochemical decay of one or both of the metallic (or ceramic) surfaces in contact, the study of compacted oxide layer glazes is sometimes referred to as part of the more general field of high temperature corrosion.

The generation of oxides during high temperature sliding wear does not automatically lead to the production of a compacted oxide layer “glaze”. Under certain conditions (potentially due to incorrect conditions of sliding speed, load, temperature, or oxide chemistry/composition), the oxide may not sinter together and instead the loose oxide debris may assist or enhance the removal of material by abrasive wear. A change in conditions may also see a switch from the formation of a loose, abrasive oxide to the formation of wear-protective compacted oxide glaze layers and vice versa, or even the reappearance of adhesive or severe wear. Due to the complexities of the conditions controlling the types of wear observed, there have been a number of attempts to map types of wear with reference to sliding conditions in order to help better understand and predict them.

*Wear scar due to adhesive friction simulation—normal techniques used for simulation and their merits and demerits.*

Study of the structures and properties of a wide range of substances could be done using molecular dynamics. It throws light directly on the atomic level information. Many theories could be experimentally proved based on the motion of atoms. While simulating molecular motion dynamics, the initial and subsequent conditions are very critical. A proper empirical potential is of great interest while molecular dynamic simulation.

The author's own experience has proven data using data logger potential for a system of interest, which reveals clearly that wearless friction is quite possible. In molecular simulations, wearless friction and friction with wear are both possible to simulate at the atomic level. It gives an account of the chemical reactions that take place during dynamic motion of molecules.

### **Molecular Level Hydrogen as a Lubricant**

Besides the traditional empirical potentials, bond order potential can simulate bond breaking and formation processes. To study material properties accurately with a consistent approach is to incorporate nonbond interactions into the bond order potentials. Some of the surfaces of hard material with magnitude of adhesion wherein the adhesive friction is strengthened by a number of high friction are reconstructed into reduced friction or adsorbate passivation (low friction) of the surface bonds. The links of the unsaturated bonds generated from high friction adhesive force, while heating, which is passivated by benign gases like hydrogen that is chemisorbed, causes the radical increase or decrease in adhesion and friction.

The high strength and polycrystalline nature of materials employed will have high strength and fracture toughness with high thermal conductivity and such surfaces readily dissipate high frictional heat from the functional areas. Such surfaces normally exhibit higher lubricating surfaces at high temperatures.

The reactive hydrocarbon potential using molecular dynamics simulation can study wearless AFM-measured friction forces at the atomic level and the friction coefficient measured under full hertzian contact conditions. The reactive potential also permits the study of lubricative surface adsorbates.

Electron energy loss spectroscopy requires conductive samples of high surface finish to avoid charging effects and to increase electron reflectivity at low electron energies. Surface charging causes shifts in the AES and XPS energy peaks in a surface with increased purity (lower sp<sup>2</sup> content). IR can reveal hydrogen, oxygen, or hydroxyl moieties bonded to carbon through covalent bonds.

Surface chemical information can throw light on COF. There is a substantial increase in the COF at elevated temperatures on a hard surface, which is attributed to dangling of the surface bonds on the desorption of adsorbates, combined with wear that induces tearing of the counterfaces. There is a shift in the COF increase peaks to higher temperatures going from vacuum to low partial pressures of hydrogen test atmospheres. This shift is in accordance with the Le Chatelier principle that if a reaction (the desorption of the adsorbate) results in a gas (e.g. H<sub>2</sub>)

as a product, increasing the partial pressure activity of this gas in the tribometer chamber will retard the reaction, while desorption occurs at higher temperatures.

### ***1.2.3 Mechanisms Manifesting the Dynamics***

Conceptually, the BFMC “system” may be described as a group of different materials containing interacting components which do not react or dissolve to form a third compound or a complex. Together with the relationships among them it makes them permit the identification of a boundary-maintaining entity or process.

### ***1.2.4 BFMC System—Process***

For purposes of better presentation and understanding of BFMC in this chapter, a system is referred based on the definition of Russell Ackoff’s suggestion that it be a set of two or more interrelated elements with the following properties:

1. Each element has an effect on the functioning of the whole system.
2. Each element is affected by at least one other element in the system.
3. All possible subgroups of elements also have the first two properties.

### ***1.2.5 Definition of BFMC System***

In the most basic definition, a system is a group of interacting components that conserves some identifiable set of relations with the sum of the components plus their relations (i.e., the system itself) conserving some identifiable set of relations to other entities (including other systems). A system is less a thing than a pattern.

By substituting the concept of “element” with that of “component,” it is possible to arrive at a definition that relates to BFMC system or system of any kind (e.g., science, mathematics). In each case, a whole is made up of interdependent components in interaction, which could be identified as the system.

This definition specifies a limited set of entities in the real world. If any set of events in the physical universe is to conserve an identifiable set of internal relations it must be capable of at least temporarily withstanding the statistical outcome of disorganization predicted by the second law of thermodynamics. This law states that “entropy always increases in any closed system which is not in equilibrium, and remains constant for a system which is in equilibrium.”

### ***1.2.6 Properties of the System***

#### *Systems Theory Model*

Referring to the method proposed by the systems theory model, complex entities are created by the multiple interactions of components by abstracting from within certain details of structure and components, and their concentration. The dynamics that define the characteristic functions, properties, and relationships are internal or external to the system.

### ***1.2.7 Dynamical and Complex Systems***

- To describe complex systems with its blind play of atoms, which, in mechanistic and positivistic philosophy, appears to represent the ultimate reality, with life as an accidental product of physical processes and mind as an epiphenomenon. Always naturally quoted it was chaos when, in the current theory of evolution, the living world appeared as a product of chance, the outcome of random mutations, and survival of all in the mill of natural selection. In the same sense, BFMC, in the theories of behavior could be mentioned after analysis, is considered as a chance product of naturally occurring materials mixture. Nurturing them results in a mixture of designs and patterns.
- Developing unifying principles running “vertically” through the universe of the individual sciences, this theory brings us nearer to the goal of the unity of science in the twenty-first century.
- Systems will dissipate energy unless they are purposefully maintained by an outside agency; thus there must be organizing forces or relations present which permit the conservation of its structure and function. Internal relations in an entity not possessing such characteristics tend to degrade until a state of thermodynamic equilibrium is reached.
- BFMC systems share the same common characteristics. These common characteristics include the following:
- BFMC systems have a structure that is defined by its components and processes.

Systems are generalizations of reality.

1. BFMC systems tend to function in the same way every time exhibiting nonlinear nature. This involves the inputs and outputs of materials (energy and/or matter), which is then processed causing it to change in some way.
2. The various parts of a BFMC system have functional as well as structural relationships between each other.
3. The fact that functional relationships exist between the parts suggests the flow and transfer of some type of energy and/or matter.

4. Systems often exchange energy and/or matter beyond their defined boundary with the outside environment, and other systems, through various input and output processes.
5. Functional relationships can only occur because of the presence of an external driving force.
6. The parts that make up a system show some degree of integration—in other words the parts work well together.

There are at least three kinds of properties one can find within the boundary of a BFMC system.

Elements—are the kinds of parts (things or substances) that make up a system. These parts may be atoms or molecules, or larger bodies of matter like sand grains, fibers, organic, inorganic, etc.

### ***1.2.8 BFMC Systemic Attributes***

BFMC systemic attributes are characteristics of the elements that may be perceived and measured. For example: quantity, size, color, shape, geometry, volume, temperature, and mass.

Relationships—are the associations that occur between elements and attributes. These associations are based on cause and effect.

We can define the state of the system by determining the value of its properties (the elements, attributes, and/or relationships).

### ***1.2.9 Complex Systems—Definition***

BFMC systems could be brought under the purview of the groups and classifications and is classified as follows:

There are several groups and classifications of types of systems. Some of the classifications or types include:

**Isolated System**—a system that has no interaction beyond its boundary layer. Many controlled laboratory experiments are of this type of system.

**Closed System**—is a system that transfers energy, but not matter, across its boundary to the surrounding environment. Our planet is often viewed as a closed system.

**BFMC as an Open System**—transfers both matter and energy which can cross its boundary to the surrounding environment. Most ecosystems are examples of open systems.

**Morphological System**—this is a system where we understand the relationships between elements and their attributes in a vague sense based only on measured features or correlations.

In other words, to understand the form or morphology a system has, based on the connections between its elements. We do not understand exactly how the processes work to transfer energy and/or matter through the connections between the elements.

**Cascading System**—this is a system where we are primarily interested in the flow of energy and/or matter from one element to another and understand the processes that cause this movement. In a cascading system, we do not fully understand quantitative relationships that exist between elements related to the transfer of energy and/or matter.

**BFMC as a Process-Response System**—this is a system that integrates the characteristics of both morphological and cascading systems. In a process–response system, one can model the processes involved in the movement, storage, and transformation of energy and/or matter between system elements and we fully understand how the form of the system in terms of measured features and correlations.

**BFMC** could also be more appropriately classified as an **Open, Process-Response—Control System**—a system that can be intelligently manipulated by us.

**Ecosystem**—is a system that models relationships and interactions between the various biotic and abiotic components making up a community or organisms and their surrounding physical environment.

Stochastic methods could be used for the analysis of test data related to the design of brake pad compositions. The friction and wear test data are analyzed by MRA (Multiple Regression Analysis) and the effect of percent volume of the components on the friction and wear characteristics could be obtained quantitatively in the form of the standard regression coefficients. The analytical results concerning the effects on component materials on friction and wear characteristics correspond well to the knowledge we gain through experience. It has been found that the standard regression coefficients, particularly those for the wear, are sensitive to the experimental conditions. This finding corresponds to the lower reproducibility of the results of the wear test. The data are then used to design the composition of brake pads. Optimization could be done using a GA (Genetic Algorithm). The predicted friction data of the designed brake pads should agree well with the test data. The calculation time will normally be about 1/700 of that by an alternative random search method.

### ***1.2.10 Complex Systems***

Complex systems from nonlinear dynamics are organized into their systems but their behavior cannot be predicted.

A macro level analysis of unstable equilibrium conditions and how the evolution of the process could be mathematically expressed with a set of linear equations. For instance, the biological human brain is one such complex system, and friction material composite (BFMC) is another advanced material complex system of a different nature. Linear systems have control on stability. In a friction material composite, input is never proportional to output for a given set of parameters. Between linear and nonlinear differential equations derived for BFMC, if it is linear in its unknown

function with its derivatives even in the case of nonlinear known functions which appear as coefficients. Nonlinear systems are not random but appear to be chaotic for simple change in the physical system in one part and can create complex system throughout like in a BFMC system. In a linear equation  $f(x) = C$ , assuming  $x$  could be a function of friction coefficient wherein association of an element say zirconium to a range with each element in a domain or it could be defined as a field. It could be an evolutionary function which can create discrete dynamic systems.

Time dependence of a point in geometrical space like the contents of a BFMC. Continuously varying quantities modeled by functions and their rates of change in space and time could be expressed as derivatives.

With a typical time varying factor in a motion of a vehicle with its velocity variations, Newton's laws allow one (given the position, velocity, acceleration, and various forces acting on the body) to express these variables dynamically as a differential equation for the unknown position of the body as a function of time. In some such cases, this differential equation (called an equation of motion) may be solved explicitly.

To recall differential equation, it is a mathematical equation for an unknown function (dependent variable) which is a function of single/multiple independent variable of one or several variables that relates the values of the function and its derivatives of various orders.

The second volume of this book series covers self-lubrication and various issues related to the reduction of friction. Friction and wear during sliding or rolling of solid surfaces are universal phenomena and they reflect the tendencies of energy to dissipate and material to deteriorate, which are consequences of the second law of thermodynamics. In general, solid surfaces in relative motion require lubrication, which dramatically reduces the extent of friction and wear. The situation when no external lubrication is required is called self-lubrication. There are many mechanisms of self-lubrication ranging from coatings to embedding lubricant into the matrix of a composite material, which are self-organized in situ tribofilm surfaces.

If we were to define frictional force in a simpler way, frictional force is the interaction between the charged particles of two bodies near the surfaces of contact. In the atomic scale, the surfaces are highly irregular as shown in the following atomic force microscopy (AFM) pictures.

Refer atomic force microscopy pictures from Figs. [1.6](#), [1.7](#), [1.8](#), [1.9](#) and [1.10](#).

*Equipment*—Dimension 3100 model Veeco

AFM—Method of measurement

Contact mode	Silicon nitrate tip
Resolution	40–50 nm
Scan area	70 $\mu\text{m}$
Method	Image scanning followed by laser detector deflection of the tip
Measuring device	Photodetector to measure the deflection of the tip
Software	Image analysis software is used

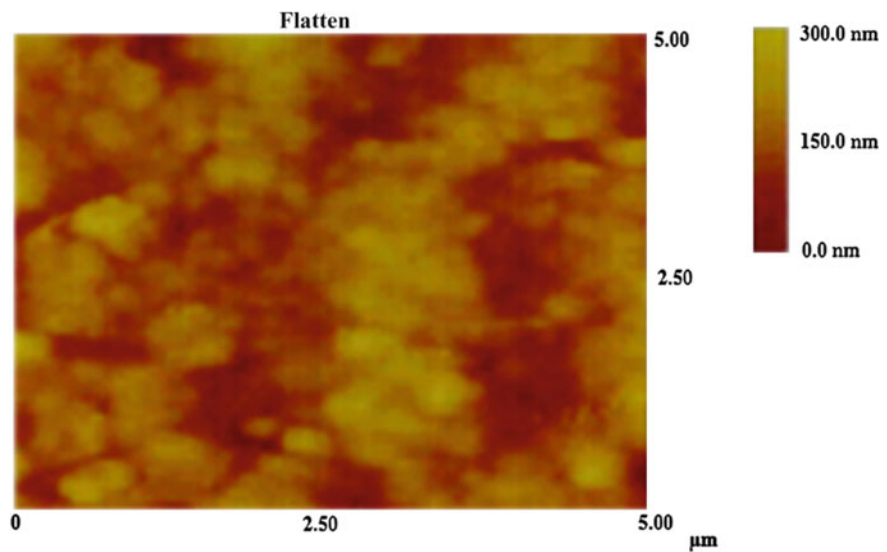


**Fig. 1.6** AFM picture of a composite railway brake block surface. Digital instruments, nanoscope, scan size: 5.000 μm, scan rate: 1.052 Mz, number of samples: 512, image data height, data scale 300 nm, engage *x* pos—19783.4 μm, engage *y* pos—42151.3 μm, *X*—1.000 μm, *Z*—507.029 nm/div

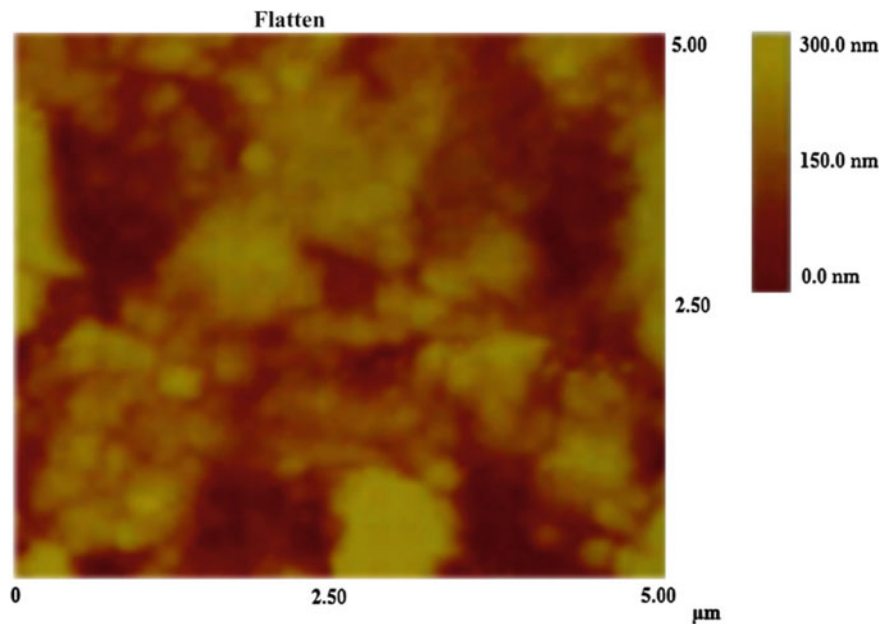


**Fig. 1.7** AFM picture of a composite railway brake block surface. Digital instruments, nanoscope, scan size: 5.000 μm, scan rate: 1.052 Mz, number of samples: 512, image data height, data scale 182 nm, engage *x* pos—19783.4 μm, engage *y* pos—42151.3 μm, *X*—1.000 μm, *Z*—507.029 nm/div

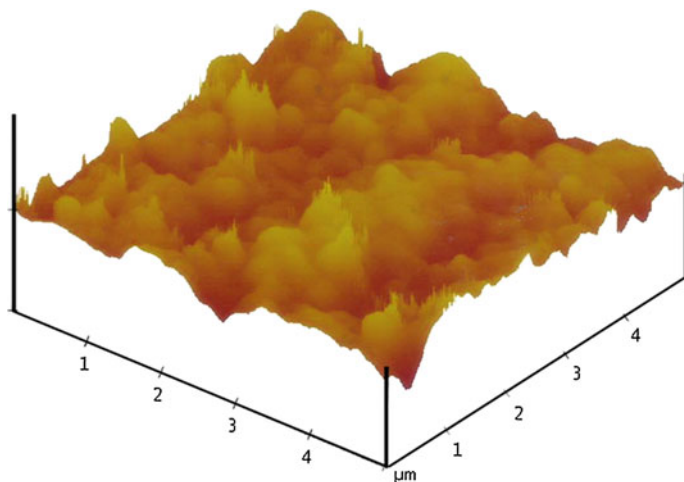


**Fig. 1.8** AFM picture of a composite railway brake block surface. Digital instruments, nanoscope, scan size: 5.000  $\mu\text{m}$ , scan rate: 1.052 Mz, number of samples: 512, image data height, data scale 507.0 nm, engage  $x$  pos—19783.4  $\mu\text{m}$ , engage  $y$  pos—42151.3  $\mu\text{m}$ ,  $X$ —1.000  $\mu\text{m}$ ,  $Z$ —507.029 nm/div

In AFM mode, the probe's tip rests directly on the sample [20], allowing the frictional force to be measured as it moves over the sample's surface atoms. In (STM) Scanning Tunneling Microscope, the probe hovers over the surface close enough, so that the electrons in the sample's atoms begin to “tunnel” or generate an electric current across the gap between the tip and the sample. Both use a probe that tapers to a single atom at its tip, but they perform different tasks. The deflections give the friction coefficient equivalent that could be measured accurately at high resolutions.

The AFM scan reveals the phase changes in two dimensions. Nanoparticle inclusions of spherules or globules are observed with two different material constituents as seen in rail brake block samples in Figs. 1.6, 1.7, 1.8 and 1.9.

At higher resolutions with the range of two-dimensional and three-dimensional scans, one can deduce dispersion of phases containing different elements with differing atomic numbers. Further, with the support of XRD bulk phase composition with surface level distribution of  $Z$  elements are deduced. Overall with precise data from XRD, EDAX, AFM, and SEM (secondary electron probe mode for surface topography in back scattering mode) one can deduce and establish friction accurately.

Note: Range of electrical voltage variation measured for scan based on the deflections gives the friction coefficient equivalent (Fig. 1.11).

To understand why friction is independent on the surface area we need a microscopic view of the contact. Practical surfaces are generally rough, and they only touch through contact “points” or “junctions”.

Figure 1.12b shows two rough surfaces sliding past each other. When the load is applied it increases the asperities and becomes flattened by elastic deformation. This increases the effective contact area, resulting in friction.

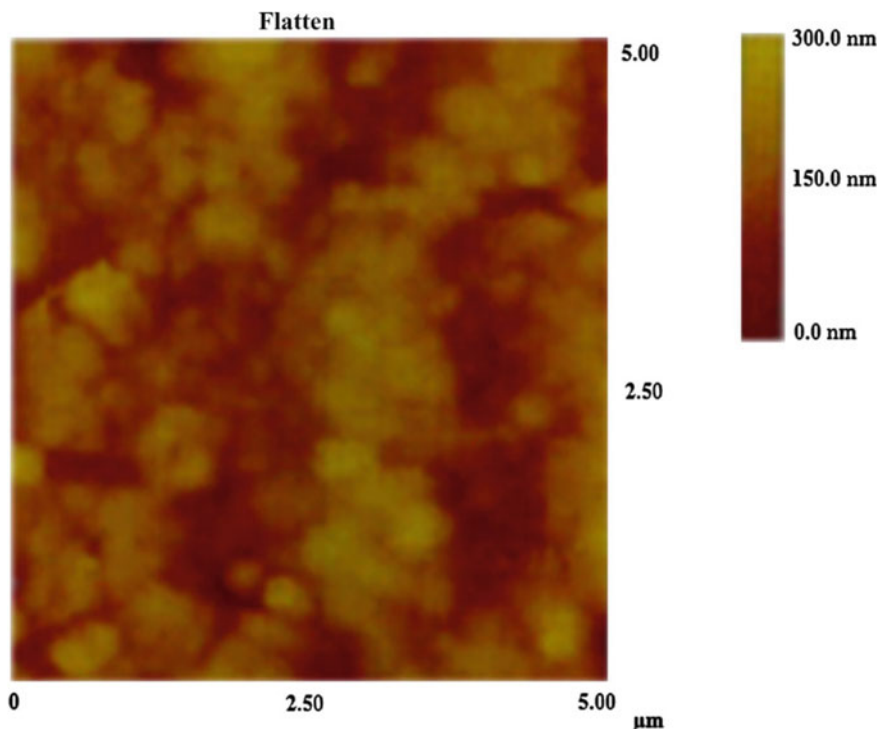


**Fig. 1.9** AFM picture of a composite railway brake block surface. Digital instruments, nanoscope, scan size: 5.000  $\mu\text{m}$ , scan rate: 1.052 Mz, number of samples: 512, image data height, data scale 507.0 nm, engage.x pos—19783.4  $\mu\text{m}$ , engage.y pos—42151.3  $\mu\text{m}$ , X—1.000  $\mu\text{m}$ , Z—507.029 nm/div

At the contacting surface the mechanism of tribo-oxidation plays a crucial role in stabilizing the friction performance of the system. The fine microstructure and homogeneous chemical composition of friction layers on both brake pad and rotor suggest that the iron oxide contains inclusions of solid lubricants on a very fine scale in the form of nanoparticles. A field ion microscope (FIM) can characterize tips down to the atomic scale.

Briefly describing, a FIM consists of a very sharp metal tip held in a low pressure He atmosphere at high potential with a grounded phosphorus screen a short distance away (approx. 5 cm). He atoms are ionized by the strong field from the tip and travel along the field lines to the grounded screen. Because the density of field lines is highest at points with the smallest radii of curvature (the atoms at the end of the tip), more ions are created there and the location of the atoms is projected onto the grounded plate. FIM images are 2-D projections of the three-dimensional tip and from the rings of atoms the crystalline planes can be reconstructed.

Additionally, by increasing the voltage on the tip, it is possible to controllably remove the outer ring of atoms by field evaporation and change the size of the tip.

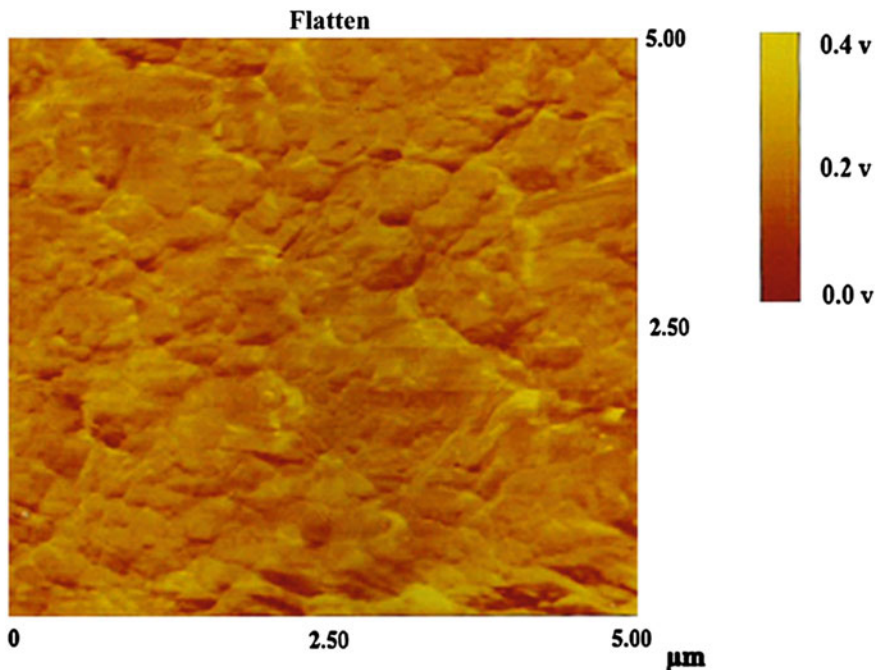


**Fig. 1.10** AFM picture of a composite railway brake block surface. Digital instruments, nanoscope, scan size: 5.000  $\mu\text{m}$ , scan rate: 1.052 Mz, number of samples: 512, image data height, data scale 400 mv, engage  $x$  pos—19783.4  $\mu\text{m}$ , engage  $y$  pos—42151.3  $\mu\text{m}$ ,  $X$ —1.000  $\mu\text{m}$ ,  $Z$ —507.029 nm/div

Using FIM in conjunction with an FFM, we will not only know the contact area but also the crystallographic orientation of the tip with respect to the sample. We can study the frictional dependence of commensurate and incommensurate lattices between tip and sample and the dependence of friction on scan direction. In addition, we will be able to change the size of the asperity in situ and look at the transition from microscopic, “single atom” friction to “macroscopic” friction.

Reviewing the historical and modern understanding of the most basic equation of friction, Amontons’ law describes phenomena that were already understood and studied by Leonardo da Vinci 500 years ago. This law states that for any two materials the (lateral) friction force is directly proportional to the (normal) applied load, with a constant of proportionality, the friction coefficient that is constant and independent of the contact area, surface roughness, and sliding velocity. No theory has yet satisfactorily explained this surprisingly general law; all attempts have been made to model which are system dependent.

Reviewing the experimental evidence finds, for example, that the same friction coefficient is often measured for the same system of materials with junctions whose areas differ by more than six orders of magnitude. The trend through molecular dynamics (MD) simulations agree with the recent and past experiments and with

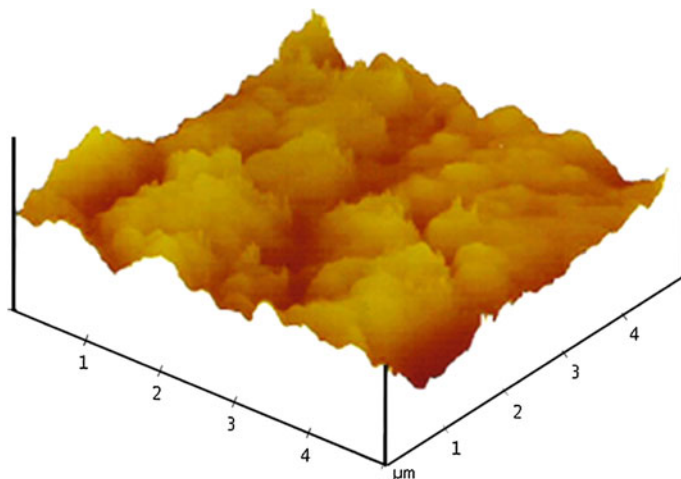


**Fig. 1.11** AFM picture of a composite railway brake block surface. Digital instruments, nanoscope, scan size: 5.000  $\mu\text{m}$ , scan rate: 1.052 Mz, number of samples: image data—friction, data scale 595 nm, engage x pos—19783.4  $\mu\text{m}$ , engage y pos—42151.3  $\mu\text{m}$ , X—1.000  $\mu\text{m}$ , Z—507.029 nm/div

Amonton's law, that the local energy-dissipating mechanisms are not merely "mechanical," as assumed in most models, but "thermodynamic" in nature, like miniature irreversible compression–decompression cycles of the trapped molecules between the surface asperities as they pass over each other. The MD analysis reveals that for such dynamic, nonequilibrium, energy-dissipating processes, a proper statistical description can be formulated through the use of the Weibull distribution of the local friction forces, similar to the Boltzmann distribution for classical systems at equilibrium.

Molecular dynamics simulated models can further reveal very useful characteristics of surface molecules and their heat dissipation changes that they exhibit on a scale ranging from  $10^{-3}$  to  $10^{-12}$  or even  $10^{-15}$ . Trapped molecules between the surface asperities and their irreversible behavior can throw light on the friction stability or instability over a range of scanned asperitic contacts.

### ***1.2.11 Definition of Composite Materials***

Composite materials are an admixture of a variety of structurally complementary distinct materials, which may be inorganic, organic, polymeric, metallic in nature. The individual components neither react with each other nor do they dissolve to form a new compound. However, they all act together to get the required characteristics of a composite that functionally and structurally has distinct properties not present in any individual component used. The BFMC mixture bears great significance on the sequence and time of addition of ingredients mixed to make a composite mixture in a

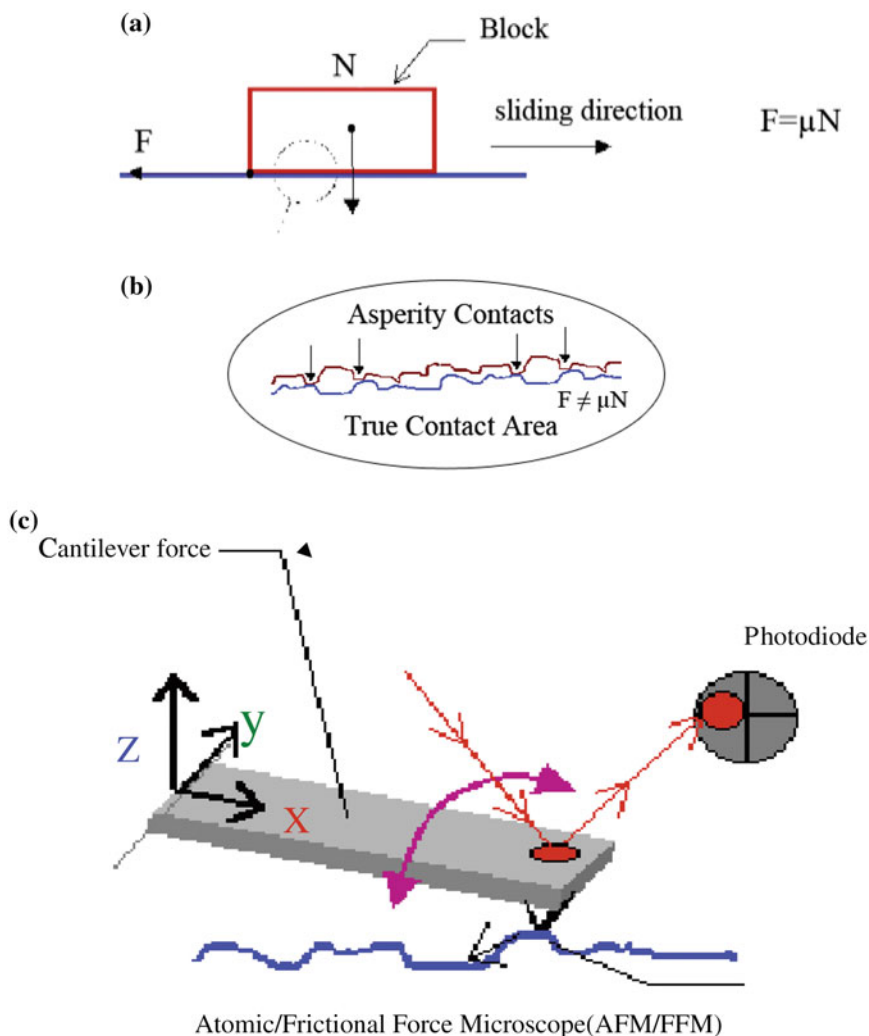


**Fig. 1.12** **a** Macroscopic friction, **b** microscopic friction and **c** AFM/FFM tip, the motion of the Cantilever is recorded via a split quadrant Photodiode

specified mixer like a Lodge mixer. Mixer has a great bearing on the characteristics of the end performance in a safety component like a brake pad liner. Here, the entire sequence needs to be carefully evaluated and issues addressed while mixing, without disturbing the grain size, geometry, shape, particle interfaces, etc. This requires extensive experience of the formulation scientist who designs the formulation with the respective processes uniquely inbuilt into the design.

In nature, bone is a typical example of a biosynthetic composite that constitutes phosphorous fibers with a binder collagen, a polymer that binds them together.

### ***1.2.12 Friction Material Composites (FMC)***

FMC could be classified under a group of composite materials that on contact with the opposing contacting surfaces produce a frictional force with two opposing forces resulting in a torque.

### ***1.2.13 Brake Friction Material Composites (BFMC)***

The group of friction materials which works in different brake systems to stop vehicles, equipment, machines, and others because of the frictional force, all could be classified as brake friction material composites.

### ***1.2.14 Brake Friction Material Composites (BFMC) with Metal Matrix***

A matrix is a monolithic material with embedded reinforcing materials that are continuous in nature. A matrix acts as a path to any point in the material which has no sandwichment or entanglement.

In a BFMC, we find that reinforcing materials are dispersed into a single metal or a multimetal matrix such as nickel and steel, nickel and brass, and steel and bronze based on the end property requirements. In some cases, reinforced surfaces are coated to prevent a chemical reaction with the matrix. For example, carbon fibers carrying systems if they contain aluminum content tend to react. In the case of BFMC, the reinforcing materials are discontinuous and are used in the form of “whiskers,” short fibers, or particles, which are anisotropic, and their strengths vary based on the reinforcement direction and alignment.

### ***1.2.15 Brake Friction Material Composite (BFMC) with Polymer Matrix***

Among the several groups of materials working together, polymeric matrix acts as a binder that binds the various ingredients together, based on its inherent binding adhesive strength characteristics and acts as a key role player.

In principle, the binding property exhibited by the binder polymer acts as a good controller of mechanisms of friction and wear. It governs performance-related issues such as noise, grabbing, and judder. Conventionally, phenolic resins have been made from cashew nut shell liquid, which possesses excellent fade characteristics by virtue of its cardanol and anacardic acid content. These two main contents largely depend on the source and terrain on which the cashews grow.

Other thermosetting polymers such as aralkyl-modified phenolic novolac, epoxy modified phenolic novolac, boron modified, phosphorous modified melamine modified, epoxy cashew modified, rubber modified all work in different formulations, with an individual entity role or in different polymeric combinations. Dependability is more on the compatibility of the polymers with the systems in operation and the process selected. The synthesis of the above said modifications of phenolic resin demands good control of the reaction rate/molecular weight distribution and other chemical characteristics. Basic controls are exercised in the reaction kettle, which in turn depends on the functional groups in the polymer. End specification controls are achieved by controlling the desired flow, low free phenol content (as an impurity), percent use of hexamethylene tetramine as a cure content, gelling time, etc. All these parameters determine the effective control on friction and performance based on their usage ratio in a BFMC system.

### ***1.2.16 Brake Friction Material Composite Multimatrix***

Friction material composite design works with multimatrix materials that are polymeric and metallic in nature. These constituents enhance the required physical, mechanical, thermal, and friction characteristics while trying to meet the technical specification requirements of the brake system of which BFMC is a part.

## **1.3 Basic Issues of Friction Material Particle Interphases**

The properties of friction material composites largely depend on the interfacial characteristics and are quite complex, as a multimatrix, multicomponent system. The interfacial strength determines how efficiently the stress is transferred to the fibers in the case of fiber dimensional variations. In effect, it controls the fracture toughness and the fatigue resistance, generally derived from mechanical and chemical bonding. Important properties such as elastic modulus in several different directions, tensile strength, density, coefficient of thermal expansion, thermal and electrical conductivity properties are all estimated from the fiber arrangement, fiber properties, volume fractions of the matrix, and reinforcing materials.

The rule of mixtures does not apply here as the properties depend on the spatial arrangement and disposition [64]. Friction material composites are also susceptible to thermal fatigue failure. To minimize thermal fatigue damage with failure, the

difference between the thermal expansion coefficients of the matrix and the fiber materials must be minimized in the system design. To circumvent this issue, oxide layers act as a flexible fiber coating and help ease the thermal stress at the interfaces.

## 1.4 Disk Pad Rotor and Caliper Assembly

See Fig. 1.13.

## 1.5 An Account of Frictional Force

Frictional forces are quite complex every time we measure with change in conditions of surfaces of contact, and every time we brake. Let us take the example of drag on an airplane flying through the air.  $F \sim cV^2$  air rushing over the wings, the swirling in the back, the changes that go on around the fuselage and because of that many other attributes that change. From the original forces of law, we all know, drag force constant times the square of the velocity is a simple fundamental definition.

Drag friction depends nearly linearly on the velocity. Drag increasingly becomes nearly proportional to the square of the velocity ( $F = CV^2$ ). With increasing velocity, the change in coefficient becomes small and negligible.

Bodies having dry, sliding friction slide on one another to maintain the motion and cause frictional force. Its origin is very complicated. Both surfaces of contact are irregular in an atomic plane. There are many points of contact, where the atoms seem to cling together and then, as the sliding body is pulled along, the atoms snap apart and vibration ensues. Power is consumed with no loss of energy and friction originates in lifting the slides over the crests and irregularities.

Power loss is that factor which has the sliding object over the crests and troughs when irregularities snap, deformation of crests takes place and generates waves with atomic motions, generating heat in the two bodies.

The force needed to overcome friction and to drag one object over another depends on the normal force perpendicular to the surface between the surfaces that are in contact.

Actually, to a fairly good approximation, the frictional force is proportional to this normal force and has a more or less constant coefficient  $F = \mu n$  where  $\mu$  is called the coefficient of friction (Fig. 1.14).

There are certain practical or engineering circumstances when we need to understand the amount of force. Normal force or high speed movement becomes too high as the law fails in the case when excessive heat is generated.

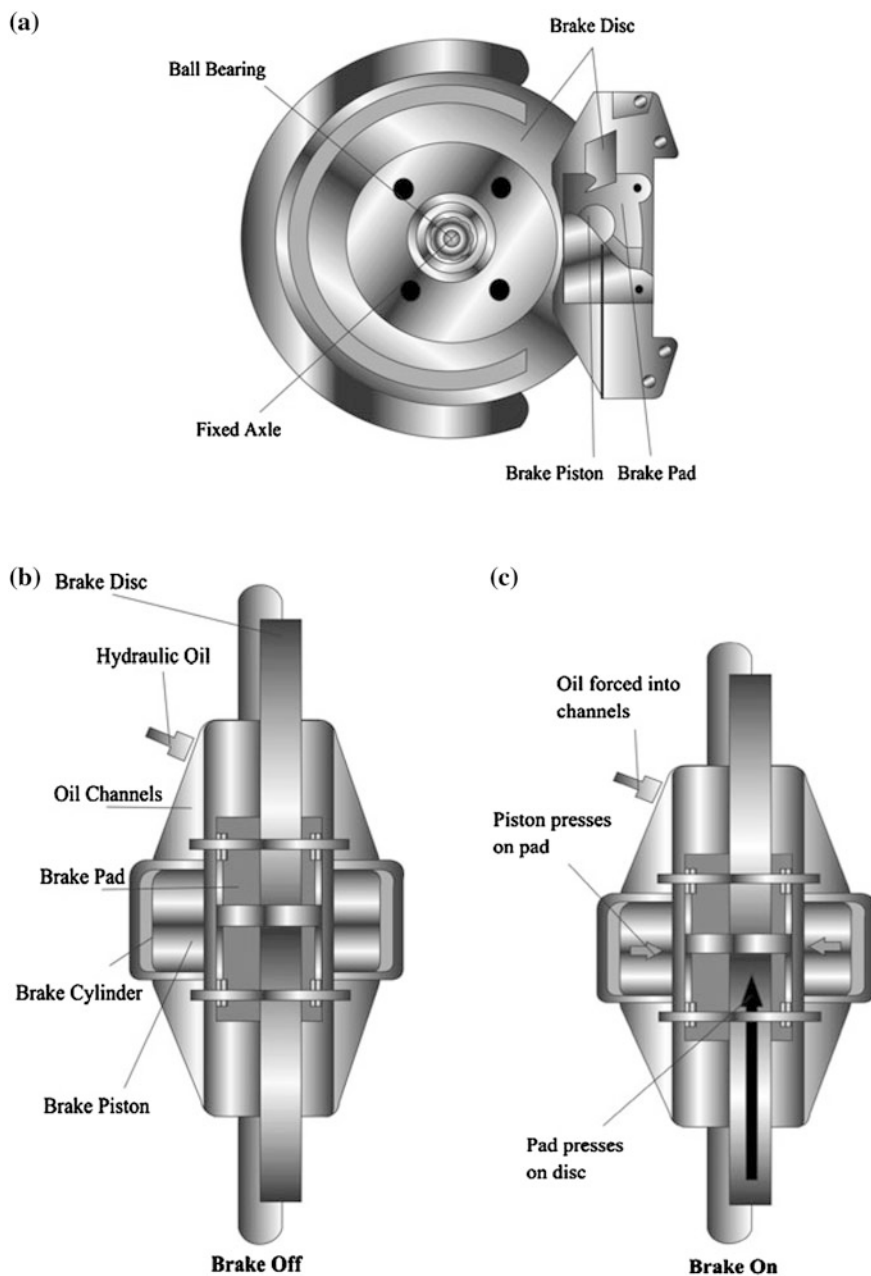
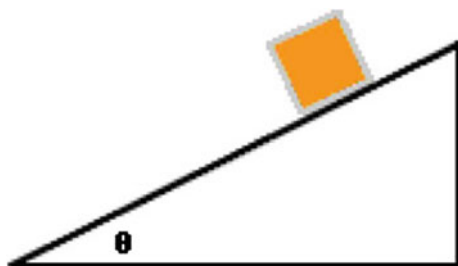


**Fig. 1.13** a Rotor disk with brake pad in contact, b brake off, c brake on

**Fig. 1.14** Force acting in a tilted plane



$$F = \mu N$$

In an inclined plane with angle  $\theta$  (Fig. 1.22) with “ $W$ ” weight of a block  $W$  acting on tilting it, at a steeper angle the block begins to slide down along the plane from its own weight, which is expressed as  $W \sin \theta$ . This must equal the friction force  $F$  when the block is sliding uniformly.

The component of the weight normal to the plane is  $W \cos \theta$  and this is the normal force  $N$ .  $W \sin \theta = \mu W \cos \theta$ ,  $\mu = \sin \theta / \cos \theta = \tan \theta$ . If this law is true, an object would start to slide at some definite inclination. If extra weight is imposed on the same block,  $W$  is increased in the same proportion but it still cancels out.

If  $\mu$  stays constant, the loaded block will slide again at the same slope. When the angle  $\theta$  is determined by trial with the original weight, it is found that the weight of the block will slide at about the same angle. This is true even when one weight is many times as great as the other and we can say that the *Coefficient of friction is independent of weight*. It is noticed that when the plane is tilted at about the correct angle  $\theta$ , the block does not slide steadily but in a halting fashion. At one place it may stop, at another it may move with acceleration. This behavior indicates that the frictional coefficient is roughly a constant and varies from place to place along the plane. This same erratic behavior is observed irrespective of whether the block is loaded. Such variations are caused by different degrees of smoothness or hardness of the plane and perhaps dirt, oxides, or other extraneous foreign matter. When we explain friction, the elements that cause friction are immaterial, whether it is steel, zirconium, copper, magnesium, or aluminum. Friction is not directly attributed to metallic copper, steel, aluminum, or zirconium alone but to the oxides and other impurities clinging to them.

*Friction coefficient is independent of velocity.*

To overcome friction to get something started, static coefficient of friction should exceed the force required to keep it sliding. Sliding friction is hard to prove especially with metals.  $F = \mu N$  is fairly accurate once the surfaces are standardized. In the case of coefficient  $\mu$  which is nearly independent of velocity, the apparent friction is much reduced if the lower surface vibrates very fast. At high speeds, care must be taken such that the objects do not vibrate relative to one another, because apparent decrease in friction at high speeds is often due to vibrations.

Frictional force by sliding a metal, copper, or steel will lead to spurious results because the surfaces in contact are not pure metals but mixtures of oxides and other impurities.

## 1.6 Characteristics of Molecular Forces

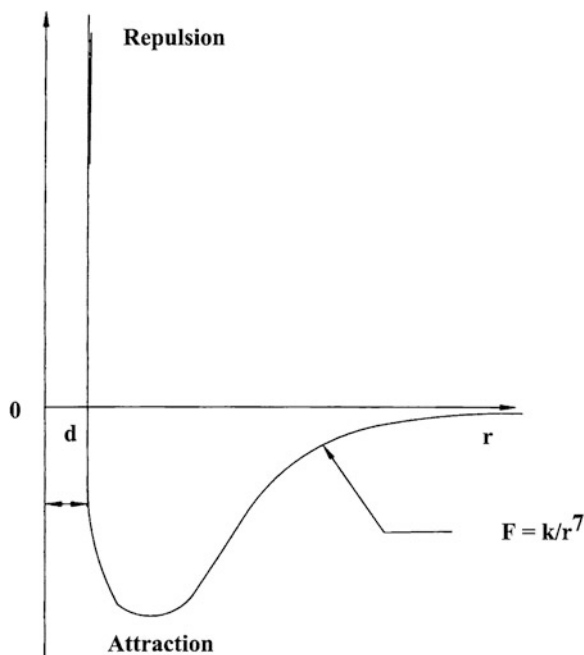
Molecular forces are the forces between the atoms and are the ultimate origin of friction. Quantum mechanics can better help understand them, explained in Volume 2. When we explain molecular forces, forces between atoms are plotted as a function of the distance “ $r$ ” between them.

For example, in water molecules the  $-ve$  charges move on the  $O^2$ ; the mean position of the  $-ve$  charges and that of the  $+ve$  charges are not at the same point. Consequently another molecule which nearly exercises a relatively larger force can be explained as a dipole–dipole force. In the case of  $O^2$ , the charges are well balanced perfectly symmetrically.  $-ve$  charges and  $+ve$  charges are dispersed over the molecule. The distribution is such that the center of the  $-ve$  charges and of the  $+ve$  charges coincides. Molecules in which the centers do not coincide are called polar molecules and the charge times for the separation between the centers is called the dipole movement. A nonpolar molecule is one in which the centers of the charges coincide.

For all nonpolar molecules, electrical forces are neutralized. It still turns out that the force at very large distances is an attraction and varies inversely as the seventh power of distance (Fig. 1.15).  $F = K/r^7$ ,  $K$  is a constant that depends on the molecule when the dipole forces are greater. When atoms or molecules get too close they repel with very large repulsion.

Look at the forces acting on the wheel. In a pure rolling motion, friction is required to stop, start, and change the motion of a wheel.

**Fig. 1.15** Molecular forces of repulsion and attraction



## 1.7 What Is a Frictional Force?

To begin with, wheel motion, wheel moving at a velocity “ $v$ ,” in a pure rolling motion, friction causes the wheel to catch and stop the sliding and slipping motion. For example, when a car spins its tires, slipping taking place, and the frictional force works to stop the spinning and causes the tires to catch and begin a pure rolling motion.

Consider the case of a body placed over a rough horizontal table. If the body is pulled by a small horizontal force, it does not move. This shows that there is another horizontal force opposing the applied pull. This opposing force is the frictional force exerted by the table on the body. When the pulling force is increased, the body starts slipping. This is due to the fact that there is a limit to the magnitude of the frictional force. When the pulling force exceeds the maximum frictional force, the body accelerates according to Newton’s law.

Therefore, an opposing force that comes into play when one body actually moves or even tries to move over the surface of another body is called friction, or the property by virtue of which a resisting force is created between two rough bodies which resists the sliding of one body over the other is called friction.

The force which always acts in the direction opposite to that in which the body has a tendency to slide or move is called the force of friction.

The maximum frictional force between two surfaces depends on the nature of surfaces and normal contact force between two surfaces. It is independent of the area of contact.

What happens in a car while braking?

When a car driver presses the brake pedal, oil is forced (Fig. 1.16) through pipes into cylinders on each side of a metal disk in the case of a disk brake system, the brake disk, attached to each of the wheels. The oil pressure pushes pistons which press the roughed brake pads against the spinning disk. Friction between the disk and pads slows the disk and the wheel and thereby reduces speed; continuous application with required pressure stops the vehicle.

## 1.8 What Happens in a Frictional Contact Surface?

When any two bodies are kept one over the other, the relative area of contact is much smaller than the total surface area of the bodies. The distance between the particles of the two bodies becomes very small at these actual points of contact when the molecular forces start operating across the surface. Molecular bonds are formed at these contact points. When one of the two bodies is pulled over the other, these bonds are broken, the materials under the bond are deformed, and new bonds are formed. The local deformation of the bodies sends vibration waves into the bodies. These vibrations finally damp out and the energy appears as the increased random motion of the particles of the bodies. The bodies thus become heated. When atoms or molecules get too close they repel with a very large repulsion (shown in Fig. 1.17).

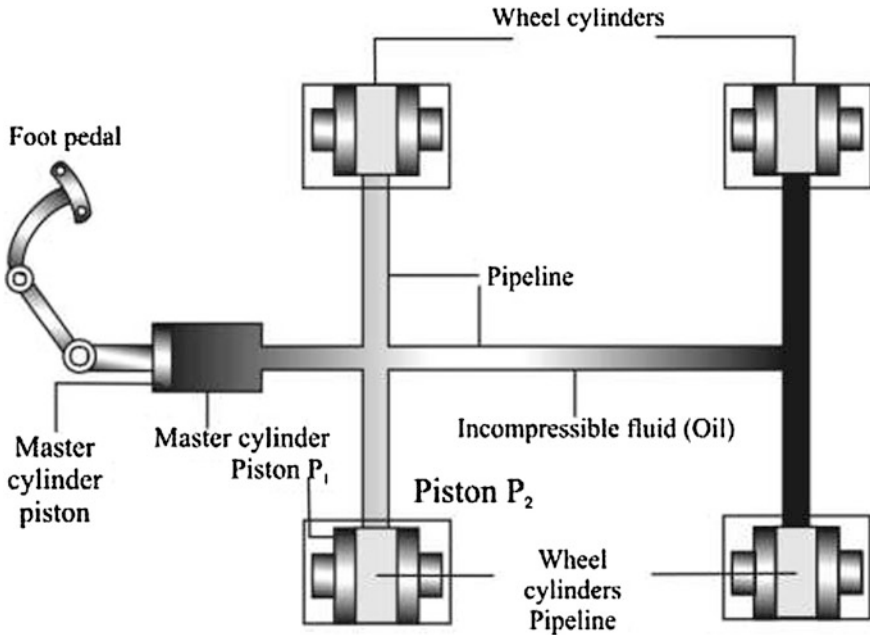


Fig. 1.16 Braking sequence from pedal to pistons, wheel cylinders

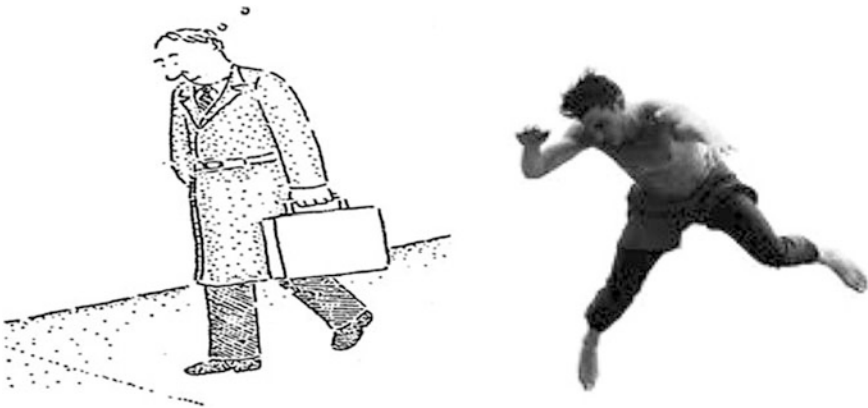


Fig. 1.17 Man slipping on the floor and falling down—large repulsion

**BFMC Wear** Wear is the volume of material lost in doing work ( $\text{m}^3/\text{MJ}$ ) and is quite complex as in situ measurements are impossible. Parameters that represent wear are mass loss, wear velocity for a given set of mechanical parameters like pressure, sliding velocity, range of temperatures in operation, besides many other respective connected parameters which are directly proportional to friction instabilities under dynamic conditions of contact in a BFMC system.

There are many situations during braking in a BFMC contact, with several mechanisms operating simultaneously in a frictional wear contact surface.

Dominant active mechanisms often mentioned are adhesive, abrasive, oxidative, delamination, fatigue, and fretting wear.

Wear can be defined as the loss or displacement of material from a solid surface (volume of material lost in doing the work— $\text{cm}^3/\text{MJ}$  by volume) as a result of mechanical action. Wear is temperature dependent and is not a constant. Material can be lost in the form of debris, whereas material can be displaced by the transfer of material from one surface to another. Wear is almost inevitable when two solid surfaces in contact move relative to each other and can appear in many ways depending on the material properties of the contact surfaces, the environment, and the operating conditions of a brake system.

The wear rate of a surface is conventionally defined as the volume or mass loss from the surface per unit distance slid or run. From an engineering point of view, wear is often classified as either mild with a low wear rate or severe with a high wear rate. Mild wear refers to processes that produce smooth surfaces, which are often smoother than the original surfaces and display minimal plastic deformation. Mild wear causes a smooth running-in of the surfaces. In the running-in process, the surface gets flattened, leading to more or less intensive wear changes to mild wear by removing the surface peaks.

However, sometimes severe intensive wear with a higher wear rate may occur, resulting in rough and scored surfaces with extensive deformation. Severe intensive wear is often associated with seizure and a severe wear situation is usually not acceptable in a braking contact as it can lead to unsafe running-in of the rotor pad contact leading to accidents.

Wear involves a number of strongly interacting mechanical and thermal processes. The heat produced by friction in BFMC contact leads to plastic flow and to thermal softening of the surfaces and of the bulk material, or to changes in the oxidation rate of the surface affecting the dominant wear mechanism and the wear rate. Hence, changes in contact conditions, such as contact pressure or sliding velocity, affect the frictional heating and high intensive wear.

## 1.9 Transfer Film Layer in a Frictional Contact Area

In the braking application, friction material sliding over the gray cast iron rotor creates a frictional heat affected layer and transfer film formation on the surface of each component. Transfer film formation and friction characteristics are extremely temperature dependent and sensitive. With increasing temperature when the transfer film is destroyed, wear increases exponentially. A decrease in wear rate will be noticed with the increase in transfer film coverage on the cast iron surface. Drop in interface temperature enhances the transfer film with an associated change in corresponding wear and friction coefficient. Frictional heat affected layer and transfer

film could be characterized using SEM, diffraction, dispersive, and fluorescence X-ray analysis besides TGA (thermo gravimetric analysis).

The nanocrystalline iron oxides provide the main fraction of superficial layers formed during braking. When we make a microstructural study, the friction layers on pads are not continuous but interrupted either by a carbon constituent or a coke or by wear troughs at the rotor surface often marked as dark bands covered by the friction layer.

The metallic layers are more pronounced after deformation than the oxide layer due to tribological stressing. The nanocrystalline friction layer can be simulated by (MCA Monte Carlo Analysis method) the behavior of the nanocrystalline friction layer during a braking application. Studies have revealed that assuming that at least part of the nanometer sized particles are released from the system eliminates the friction layer for a short time period leaving a metal on metal contact at the sites. The local coefficients of friction obtained from the MCA (Monte Carlo Analysis) simulations reveal the oxide on oxide contact quite closely to the desired mean coefficient of friction of the brake system. The oxide formation will take place more quickly than the friction layer elimination and finally for stabilization of the coefficient of friction which otherwise would increase to 1 for pure metal on metal contacts.

### **1.10 Nanostructure Metallic Materials for Enhanced Wear and Control on Friction: Ban on Copper Under the Legislation Bills SB6557 and S 346 Passed in USA and California**

The electrodeposited composite coatings helps prevent the usage of copper under the enactment of the prevention of the use of copper law by the US Government in BFMC composites. Nanocrystalline nickel matrix with 8–10 nm and titania nanoparticles 10–12 nm with copper as substrates find increased use in wear improvement. There will be drop in friction and wear with the increasing content of titania nanoparticles while sliding against steel at higher temperatures >450 °C. Matrix and dispersion particles less than 100 nm enhance the wear resistance by grain size refinement and hard inert particle dispersion [94].

The electrodeposited nickel is much harder than the conventional microcrystalline nickel. It becomes increasingly evident from research that nanocrystalline metals even at room temperature have greater strength than their microcrystalline counterparts. Similarly, ceramic nanoparticles over metal matrix based on the principles of dispersion strengthening without heat treatment have proved to have very high mechanical strength. Electrodeposition helps in various ways like low cost and is easy to operate, flexible, and large size availability, high deposition rate with full density [95].

TiO<sub>2</sub>, SiC, and ZrO<sub>2</sub> could be electrodeposited from different electrolytes in which nanoparticles are suspended. Nanocrystalline nickel with titania nanoparticles as the dispersive phase has proved to have good improvement in mechanical and corrosion resistant properties of nanocrystalline nickel coatings [97].

## 1.11 Composite Coatings for Friction and Wear Properties

X-ray diffraction method has provided vast information on the pattern of small grains of both the matrix phase and the dispersive phase of titania and nickel. The contents of the titania particles in the coatings from the diffraction results reveal higher concentration of the electrolytes. In the case of sliding friction condition for solid–solid contact, it satisfies Amonton’s laws of friction wherein friction opposes the beginning of the relative motion and friction opposes the continuance of relative motion once the motion has started.

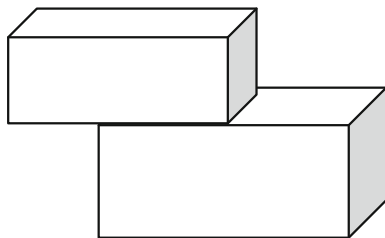
It is apparent that the coefficient of friction between nanocrystalline nickel and steel gets lowered by incorporating titania nanoparticles. Thereby microstructure design through fine particle embedment into electrodeposited metal matrix can provide huge scope for metallic lubricating coatings. Particle strengthening effect by dispersing titania nanoparticles inhibits the grain boundaries of the nanocrystalline nickel coatings and acts as an obstacle to the grain movement and grain boundary migration under cyclic normal load during sliding friction test. The titania–nickel nanocomposite coatings also lower wear than nanocrystalline nickel.

## 1.12 Geometrical Surfaces and the Forces of Friction

Frictional force is a force that resists motion and acts in the opposite direction to the motion. As the surfaces slide across each other they rub and catch together due to irregularities on the surface. In a car brake the car fully relies on friction to work effectively. Coefficient of friction is augmented in geometrically similar surface than in dissimilar surface (Fig. 1.18).

In case of similar surfaces they interlock.

**Fig. 1.18** Geometrically similar surfaces in contact



### 1.13 New Class of Quasicrystalline Materials

Quasicrystals break rules of symmetry that apply to conventional crystalline structures, and they also exhibit different physical and electrical properties. The mineral shown below exhibits how quasicrystals could form and remain stable under natural conditions.

Extensive studies [8] on atomic scale of friction and adhesion properties of quasicrystals have revealed interesting revelations. With review on tribological studies carried out in different mechanical regimes (elastic and inelastic) and at different length scales (macroscale and nanoscale) one could address the role of the surface oxide [3, 9, 66, 67] and the nature of mechanical contact in determining friction and adhesion properties. An innate relationship [1] exists between the aperiodic atomic structure of quasicrystals (Fig. 1.20) and their low friction, for both elastic [7, 13] and inelastic regimes.

Quasicrystalline materials are said to lower friction coefficient, by virtue of their periodic and aperiodic configurations both in the same crystal structure. Atoms in an aperiodic structure are ordered or regular like in a fibonacci sequence but their patterns are not regular; however, in the case of periodic structure they are regularly aligned, repeat, and normally form a three-dimensional pattern. The chemical constitutional change, which brings about a frictional variation on the surface when in contact, cannot be derived separately from periodic and aperiodic from the same material. This may have resulted in a change in friction value.

In order to have consistent coefficient of friction, an unoxidized quasicrystalline material which has counterintuitive properties (like for instance, elements which are conductive becomes nonconductive by virtue of their lattice becoming perfect) or a doping of the quasi oxidizing material would beneficially control the friction coefficient. This is mainly attributed to its underlying structure. Frictional force variations between the aperiodic and periodic direction called frictional anisotropy have dominating phononic contributions than electronic as the source of friction. (Phonons are waves or vibrations in a crystal lattice, like an atomic sound wave.) It is understood that friction along the aperiodic direction is one-eighth or in (other words 8 times larger when it is sliding along the periodic direction [16, 17] of the surface than when sliding along the aperiodic one.) as much along the periodic direction. It disappears when the surface is oxidized in air with an amorphous thin oxide film formed [5].

It results from the finding that there is strong connection between the interface atomic structure and the mechanism by which the energy is dissipated [6, 11], thereby attributing to phononic or electronic contributions or both. AFM study reveals a drop in frictional anisotropy on monolayer graphene as the load increased is attributed to ripple distortions according to the noble publication.

The increase or decrease in friction in a solid–solid contact in nonmetallic crystal contact depends more on the crystallographic plane of contact. To explain friction anisotropy of unicastal or in a multicomponent crystal surface it is quite complex to unravel the exact controls of friction mechanism [10]. In braking contact, frictional heat always accompanies the friction process. In BFMC anisotropic

friction induces anisotropic frictional heat for composites [18]. The heat intensity function depends more on the sliding direction [93].

According to the classical crystallographic restriction theorem, crystals can only possess two, three, four, and sixfold rotational symmetries. The Bragg diffraction pattern of quasicrystals, however, shows sharp peaks with other symmetry orders, such as fivefold, eightfold, tenfold, 12-fold, or even 18-fold. This can be explained by the well ordered, but aperiodic and infinite structure of quasicrystals [4, 14].

Since then, quasicrystals have been discovered in many synthetic intermetallic systems as well as in liquid-crystals, polymers, nanoparticle assemblies and micellar systems. Naturally occurring icosahedral quasicrystals, Icosahedral quasicrystals, an alloy of aluminum, copper, and iron, have recently been discovered in a river bed in Russia.

Christian Janot, Jean-Marie Dubois, and Jean Pannetier were among the first to use neutrons to study quasicrystals at ILL in 1986. They used a technique called isomorphic substitution, which gives information about specific atoms in materials containing more than one atom, like alloys. They were among the first to record a neutron diffraction pattern of Al–Mn–Si icosahedral quasicrystals (Fig. 1.19) and their work initiated [12, 15, 21] a long-term research program on quasicrystals at ILL [19].

Neutrons offer better contrast than X-rays and electrons for a number of elements, such as lithium, manganese, or nickel according to research findings. By combining X-rays and neutrons, researchers from France, the USA, and Japan were thus able to build precise atomic models of icosahedral quasicrystals such as Al–Mn–Si, Al–Li–Cu, or Al–Pd–Mn.

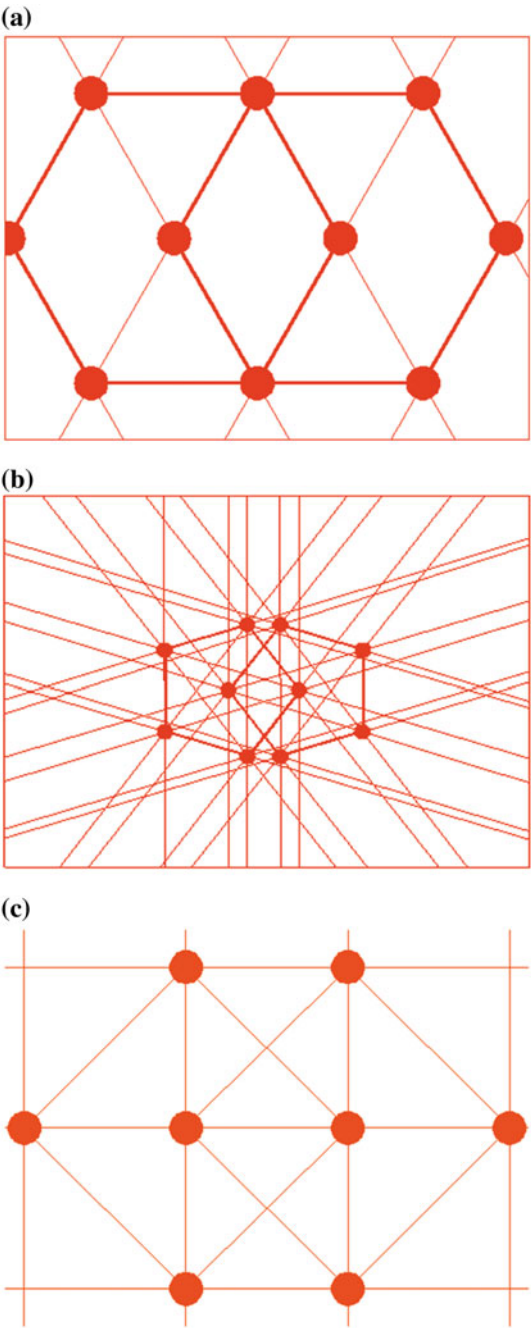
Intermetallic quasicrystals, like all complex metallic alloys, present unusual physical properties that can be exploited for a number of useful applications. Because they are poor heat conductors, they can serve as good thermal barriers, to protect metal parts from overheating. They have low friction coefficients, and trials have been carried out to replace Teflon with a quasicrystalline coating on cookware. More studies are being done to investigate this property for use in mechanical parts.

Quasicrystals are hard and brittle, but they can be used for structural strengthening, to reinforce other light alloys such as Mg-based alloys. Quasicrystals are also being studied for use as catalyzers, to replace noble metals like gold or palladium (Figs. 1.20, 1.21 and 1.22).

**Fig. 1.19** Quasi crystal—  
Al–Mn–Si



**Fig. 1.20** Periodicity. No periodicity observed in the fivefold rotational axes (b) hence it is incompatible with translational symmetry. Crystallinity and periodicity observed with equidistance in the case of 4 (a) sixfold and (c) fourfold rotational axis. Order without periodicity



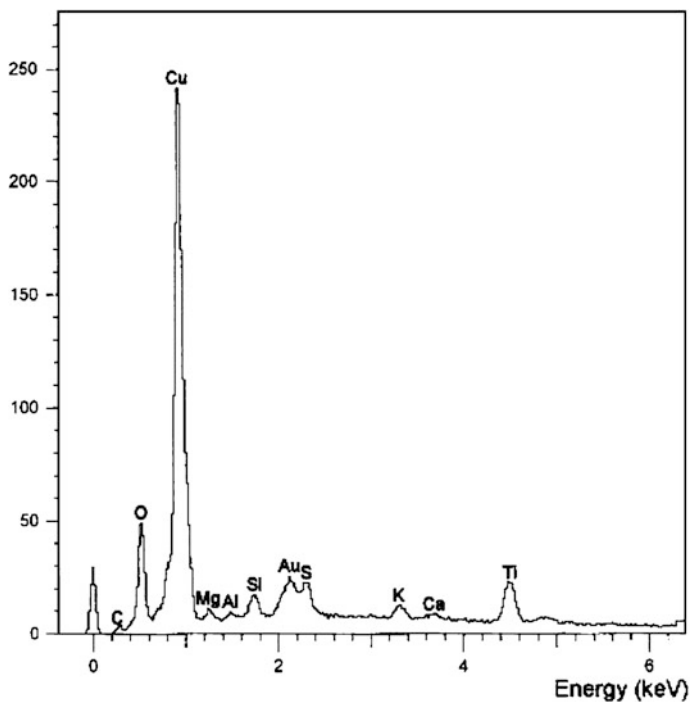
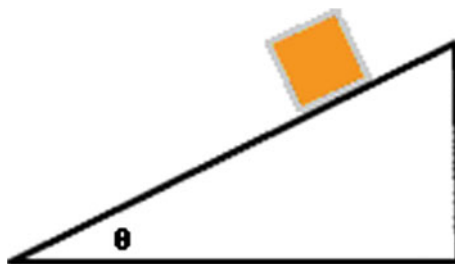


**Fig. 1.21** EDAX—energy dispersion—X-ray analysis with SEM attached. Some of the elemental peaks at different energy levels. Authors own disk pad samples studied (very useful tool for BFMC reverse engineering)

**Fig. 1.22** Object of weight  $W$  on incline of angle  $(\theta)$



#### *Calibration data*

Stroke: Energy—7.6, Resolution—61.17, Area—27984

#### *Calibration element*

Energy—6922.3, Resolution—143.96, Area—78259

Gain factor—50.032

Live time—33.6 s

#### *Sample data*

Stroke energy: 7.8, Resolution 61.30, Area—24656

Total spectrum counts: 197929, Live time is 33.6 s

System resolution: 66 eV Geometry tilt—0

ED Geometry: Elevation—45°, Azimuth—0, Entry angle—0

Accelerating voltage: 20 kV

### *Quantitative method*

ZAF (3 iterations). Analysis of all elements and normalized results.

Four peaks omitted 0.00, 0.24, 5.52 and 5.88 keV

### *Standards*

Mg	K	MgO
S	K	FeS <sub>2</sub>
K	K	MAD-10
Ca	K	Wollastonite
Ti	K	Ti
Fe	K	Fe
Cu	K	Cu
Zn	K	Zn
Zr	L	Zr
Sb	L	Sb

Energy diffraction by X-ray detector analysis acts as a microanalytical study which has the highest take-off angles, largest solid angles, and unmatched collection efficiency to identify elements with more ease. X-ray resolutions attached to EDAX as high as 10–50 mm<sup>2</sup> is normally achievable. The fully automatic light element detector with full vacuum protection, with a fully motorized control with rotating turret end-cap allows the Be window to be moved away from the line of sight of the detecting unit. Here, an open windowless configuration is utilized for ultimate in light element detection. It is an excellent material characterization system that encompasses energy dispersive spectrometry (EDS), electron backscatter diffraction (EBD), wavelength dispersive spectrometry, and micro X-ray fluorescence (Micro-XRF). EDAX is possibly the best microanalytical characterization technique for friction material composite.

Element	Spec.	Type	Apparent conce.	Stat. sigma	K ratio	K ratio sigma
Mg	K	ED	0.595	0.045	0.00986	0.00075
S	K	ED	3.996	0.082	0.07483	0.00153
K	K	ED	2.259	0.080	0.17666	0.00623
Ca	K	ED	0.778	0.075	0.02267	0.00219
Ti	K	ED	9.306	0.140	0.09306	0.00140
Fe	K	ED	1.401	0.122	0.01401	0.00122
Cu	K	ED	30.415	0.444	0.30415	0.00444
Zn	K	ED	14.459	0.419	0.14459	0.00419
Zr	L	ED	0.632	0.112	0.00632	0.00112
Sb	L	ED	0.408	0.156	0.00408	0.00156

Detailed usage of tools with EDAX, complete reverse engineering is possible for analysis and understanding of friction material composite.

Element	Speci.	Type	Inten. coren	Std corn.	Element (%)	Sigma (%)	Atomic (%)
Mg	K	ED	0.473	0.97	1.85	0.14	4.20
S	K	ED	0.886	1.02	6.65	01.5	11.42
K	K	ED	1.134	1.00	294.00	0.11	4.13
Ca	K	ED	1.103	1.00	1.04	0.10	1.43
Ti	K	ED	0.967	1.00	1.92	0.17	1.89
Fe	K	ED	1.077	1.00	1.92	0.17	1.89
Cu	K	ED	0.955	1.00	46.97	0.53	40.68
Zn	K	ED	0.959	1.00	22.24	0.54	18.72
Zr	L	ED	0.642	1.05	1.45	0.26	0.88
Sb	L	ED	0.827	1.01	0.73	0.28	0.33
					100		100.00

*Heat dissipation process with—time characteristics in a silane coated vermiculite—mica interphase in BFMC.*

Time characteristics in a silane coated vermiculite—mica interphase in BFMC analysis of multiphase systems includes consideration of multiphase flow and multiphase heat transfer. When all of the phases in a multiphase system exist at the same temperature, multiphase flow needs to be governed. However, when the temperatures of the individual phases are different, interphase heat transfer occurs.

If different phases of the same pure substance are present in a multiphase system, interphase heat transfer will result in a change of phase, which is always accompanied by interphase mass transfer. The combination of heat transfer with mass transfer during phase change makes multiphase systems distinctly more challenging than simpler systems like in silane coated mica-vermiculite interphases. Based on the phases that are involved in the system, phase change problems can be classified as: (1) solid–liquid phase change (melting and solidification), (2) solid–vapor phase change (sublimation and deposition), and (3) liquid–vapor phase change (boiling/evaporation and condensation). Melting and sublimation are also referred to as fluidification because both liquid and vapor are regarded as fluids.

In the case of braking contact with a cast iron rotor specification and the friction material contact phase the limiting torque for a given contact area relies more on the mass transfer with phase changes in the material specification (under GG classification) to deliver the required torque. Enhancing the size of the rotor contact calls for extensive understanding of the mass and phase transfer changes in the contact to deliver the limiting torque.

## 1.14 Essential Virtues of Brake Friction Material Composite

Coefficient of friction varies from about 0.30–0.60 for different types of brake linings/disk pads in an automotive or a rail braking.

Static coefficient of friction is the ratio of the limiting friction developed to the corresponding normal pressure, if two surfaces move relative to each other.

When a force is applied to pull the body and the body does not move, then the friction is equal to the magnitude of the force and acts in the opposite direction. As the body is at rest the friction is called static friction. If the force is increased, the force of static friction also increases. When the applied force exceeds a certain maximum value, the body starts moving. This maximum force exceeds a certain maximum value, and the body starts moving. This maximum force of static friction up to which the body does not move is called limiting friction. If the applied force is increased further, the body sets in motion. The friction opposing the motion is called kinetic (dynamic) or sliding friction.

Friction coefficient ( $\mu$ ), in other words damping constant ( $C$ ) in mechanical terms can analogously also be called resistance ( $R$ ) in electrical terms, just as mass ( $m$ ) is inductance ( $L$ ) or external force  $F(t)$  is expressed as electromotive force  $E$ .

Coefficient of friction is a dependent resistive force and accordingly the values vary. It is determined experimentally by force measurement required to overcome friction or by measuring the angle at which an object will slide.

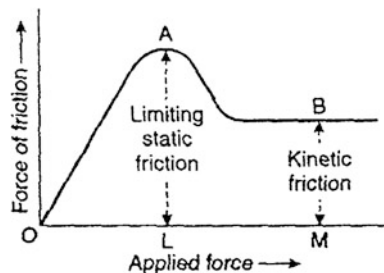
### 1.14.1 Different Types of Coefficients of Friction

The different types of coefficients of friction are static, kinetic, rolling, deformation, and molecular friction. Each has its unique coefficient of friction. Figure 1.23 shows some of the elemental peaks identified in disk pad sample of the BFMC.

#### a. Static Coefficient of Friction

Static friction is the force that holds back a stationary object up to the point of its movement. Thus, the static coefficient of friction is concerned with the force restricting the movement of an object that is stationary on a given surface of contact.

**Fig. 1.23** Shows the difference between static and kinetic friction graphically



### **b. Kinetic Coefficient of Friction**

Kinetic friction is the force holding back regular motion. The kinetic coefficient of friction is concerned with the force restricting the movement of an object that is sliding on different surfaces.

### **c. Deformation Coefficient**

The deformation coefficient of friction is the effect of forces restricting the movement of an object that is sliding or rolling on one or both surfaces that are relatively soft and deformed by the forces.

### **d. Molecular Coefficient of Friction**

Molecular coefficient of friction is the force restricting the movement of an object that is sliding on an extremely smooth surface or where a liquid, fluid is involved.

### **e. Rolling Coefficient of Friction**

It is a combination of friction of static, deformation, and molecular coefficients of friction. This coefficient of friction is normally low.

**Experiments** There are a number of experiments one can conduct to determine the coefficient of friction between two materials. There are direct and indirect measurements possible.

### **f. Direct Measurements**

An experiment to determine the coefficient of friction would be to use some force to push two materials together and then measure that force. The application of brakes in the car, or using the force of gravity to apply a weight on an object is of interest in this work.

While trying to move a car wheel when the brakes are applied, or pulling a weighted object along the floor, some simple devices measure force.

**Using the Force of Gravity** Since it is difficult to measure the force with which you squeeze, a more common way to measure the force between objects is to use the weight of one object. An object's weight is the force it exerts on another object, caused by gravity. If the weight is  $W$  in pounds or newtons, the friction equation for an object sliding across a material on the ground can be rewritten as:

$$F_r = f_r * W$$

or

$$f_r = F_r / W$$

Once you know the weight of the object you are sliding, you can use a scale to measure the force it takes to move the object.

To measure the static coefficient of friction, take the value of the force just as the object starts to move. Doing the same experiment with sliding or kinetic friction, take the reading when the object is sliding at an even velocity. Otherwise, we will be adding in acceleration force effects.

### g. Indirect Measurements

There are several indirect methods to determine the coefficient of friction. A method to determine the static coefficient of friction is to measure the angle at which an object starts to slide on an incline or ramp. A method to determine the kinetic coefficient of friction is to measure the time taken to stop an object.

**Measurement in an Incline** You can use an object on an incline to determine the static coefficient of friction by finding the angle at which the force of gravity overcomes the static friction.

Once static friction has been overcome, kinetic friction is the force holding back regular motion. This kinetic friction coefficient of friction concerns the force restricting the movement of an object that is sliding on a relatively smooth, hard surface.

**Perpendicular Force Reduced** When an object is placed on an inclined surface, the force perpendicular between the surfaces is reduced, according to the angle of the inclination.

The force required to overcome friction ( $F_r$ ) equals the coefficient of friction times the cosine of the incline angle ( $\cos(\theta)$ ) times the weight of the object ( $W$ ). There are mathematical tables that can give the values of cosines for various angles

$$F_r = \mu * \cos(\theta) * W$$

**Effect of Gravity** Note that when an object is on an incline, the force of gravity contributes to causing the object to slide down the ramp or incline. Let us call that force ( $F_G$ ), and it is equal to the weight of the object ( $W$ ) times the sine of the angle ( $\sin(\theta)$ )

$$F_G = \sin(\theta) * W$$

Tangent of angle determines coefficient.

If you put the ramp at a steep enough angle,  $F_g$  will become greater than  $F_r$  and the object will slide down the incline. The angle at which it starts to slide is determined from the equation:

$$f_r * \cos(\theta) * W = \sin(\theta) * W$$

Dividing both sides of the equation by  $W$  and  $\cos(\theta)$ , we get the equation for the static coefficient of friction  $f_r$

$$f_r = \tan(\theta)$$

where  $\tan(\theta)$  is the tangent of angle ( $\theta$ ) and equals  $\sin(\theta)/\cos(\theta)$ . There are mathematical tables for determining the tangent, sine and cosine of various angles.

**Calculation** For example, if you put an object on an inclined surface and changed the angle of the inclination until the object started to slide and then measured the

angle of the inclination, you could determine the coefficient of friction between the object and the inclination. If the angle was  $30^\circ$ , then the tangent of  $30^\circ$  is about 0.58. That would be the static coefficient of friction in this case. Even if you increased the weight on the object it would still slide at  $30^\circ$ .

### h. Time Element

You can also use a stopwatch to determine the kinetic or rolling coefficient of friction. But it is not easy to do. If you have an object moving at some velocity “ $v$ ” and you let it roll or slide along a surface until it stopped, you could then measure the time “ $t$ ” it takes to stop to determine its coefficient of friction.

From the force equation,  $F = m * a$ , where  $a$  is the acceleration. Since the object is starting at some velocity  $v$  and decelerating until  $v = 0$ , then the force of friction can be written as:  $F_r = m * v/t$ .

If the object weighs  $W$  pounds, and  $W = m * g$ , where  $g$  is the gravity constant 32 ft/s/s ( $9.8 \text{ m/s}^2$ ), then the

Friction equation is:

$$F_r = f_r * W = f_r * m * g$$

Combining the two equations for  $F_r$ , we get:

$$f_r * m * g = m * v/t$$

or

$$f_r = v/(g * t)$$

Thus, if a car is moving at 80 feet per second and takes 5 s to come to a stop, its coefficient of friction is:

$$f_r = 80/(32 \times 5) = 0.5$$

(straight line inclined equally to the two axes) represents the self-adjusting nature of the force of friction. It is clear from the graph that the body remains at rest as long as the applied force does not exceed OL. Here, AL represents the limiting static friction. When the body starts moving, the force of friction drops to a value BM. This value is slightly lower than that of limiting static friction. So BM represents the kinetic friction.

When a force is applied to pull the body and the body does not move, then the friction is equal to the magnitude of the force and acts in the opposite direction. As the body is at rest, the friction is called static friction. If the applied force is increased, the force of static friction also increases. When the applied force exceeds a certain maximum value, the body starts moving. This maximum force of static friction up to which the body does not move is called limiting friction. If the applied force is increased further, the body sets in motion. The friction opposing the motion is called kinetic (dynamic) or sliding friction.

### 1.15 Test Conditions of $\mu$ -V Testing—BMI (Bismaleimide) Polymeric Matrix-Based Composite System in a Non-asbestos to Asbestos Formulations Compared

One of the test results of a sample Asbestos and nonasbestos liner for static to dynamic  $\mu$  comparison for fixing the noise is given below:

As the ratio between static to dynamic friction nears zero as in (Fig. 1.24), one would observe good resilience with higher deformation strength and no noise during braking contact. This is a typical characteristic of an NA formulation using BMI resin matrix which by virtue of its high heat resistance also gives better wear besides no noise on braking.

Equipments: Test Machine  $\mu$ -V tester, Rotor U13/R

*High burnish conditions.*

Environment: Ambient (25 °C, 60 % RH)

Speed: 100 km/h,

Pressure 196 kPa,

Rotor Temperature: 70 °C pressures on—84 °C pressure off,

Numbers—1500

*Measuring conditions:*

Rotor revolution 0–2 rpm

Low sliding speed,

Pressure 196 kPa,

Rotor temperature—60 °C,

Numbers—20 times repeat,

Environment (30 ± °C LH, 75 °C ± 5 % RH),

Test Numbers: Each 2 times (Table 1.1).

**Fig. 1.24** Static to dynamic friction coefficient drop ratio

$$\text{Dropdown ratio} = (S.\mu - D.\mu) / S.\mu \times 100$$

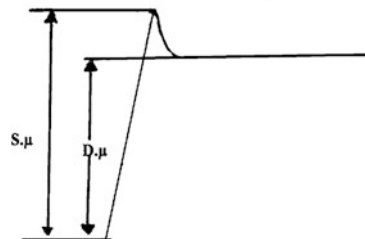


**Table 1.1** Static to dynamic  $\mu$  ratio when tested under high burnish conditions

Drop down ratio between static to dynamic $\mu$ (%)				
Asbestos based	5.6 %		Non-asbestos	0 %
	6.9 %			0 %
Average	6.3 %			0 %
Static to dynamic $\mu$ ratio (disk pad—non-asbestos to asbestos in %)				
Stops	Non-asbestos-based systems		Asbestos-based system	
	Test no. 1 (%)	Test no. 2 (%)	Test no. 1 (%)	Test no. 2 (%)
1	0	0	3.9	5.3
2	0	0	8	6.6
3	0	0	4.9	9.7
4	0	0	6.1	4.7
5	0	0	3.8	6.8
6	0	0	5.9	7.4
7	0	0	5.1	6
8	0	0	4.4	6.8
9	0	0	6.4	8.6
10	0	0	4.2	6.9
11	0	0	7.4	5.5
12	0	0	4.8	6
13	0	0	5.6	6.3
14	0	0	5	9.3
15	0	0	4.5	6.6
16	0	0	8.3	10.4
17	0	0	6.5	9.6
18	0	0	6.1	5
19	0	0	6.5	5.1
20	0	0	5.3	5.9
Average	0	0	5.6	6.9
			6.3	
Maximum	0	0	10.4	
Minimum	0	0	3.8	

**1.15.1 Coefficient of Friction—Brake Liner Fitted with “S” Cam Brake**

Assuming the contact and contacting surfaces as  $P$  and  $Q$  for a liner fitted in  $S$  cam brake, the braking force can be related to coefficient of friction by the following equation:

$$F = \mu[2MNSD/CT]$$

where  $M$  is the air pressure used to apply the brake (pounds per square inch or other equivalent units),  $N$ —air chamber size (inch<sup>2</sup>),  $S$  is the length of the level arm of the slack adjuster,  $D$  is the inside radius of the brake drum,  $C$  is the  $S$  cam brake cam radius of brake actuation (inches), and  $T$  is the roll radius of the tire. Keeping all other factors equal the friction coefficient and braking force can still vary from 10 to 20 %.

High friction means higher output from brakes resulting in shorter stopping distance. Coefficient of friction decreases with both increasing unit pressure and sliding speed between the contact, contacting surfaces.

### 1.15.2 Wear Rate

Wear rate of friction materials depends on temperature, speed, and load. In general, wear is directly proportional to applied normal load and speed. At high brake temperature, wear of the friction material may increase exponentially because of thermally induced degradation of organic resin binders and other substances. Porosity of the pads with 10–14 % are good performing pads and wears low as well. Working on such porosity levels is in the hands of the formulator and it is more of the materials design parameter.

Intrinsic wear rate on application of pressure varies with each constituent member of materials and can cause preferential wear because of certain member materials, the pressure sustenance of which is lower and to be brought down at par with other members to nullify the effect of wear, until the pressure is adjusted for thickness loss adjustment. As it carries less than its proportionate share of the load it will have a corresponding drop in overall friction level.

On the contrary, some low wear rate filler at even lower dosage volume proportion can have significant effect on friction. It depends to a larger extent on the temperature of operation conditions rather than on others.

Use of fillers for enhancing the  $\mu$  beyond 0.40–0.45 would wear the counterface and be noisy. Outside the range of 0.30–0.45  $\mu$  temperature, velocity would pose a serious issue of stability of  $\mu$ .

A high modulus favors wet friction wherein length to width ratio on wet friction could be complementary.

Wear rate increases with increase in operating temperatures and varies with each material. The nature and proportion, particle size of the fillers affect the wear rate, interaction between the various fillers, and between fillers and matrix. There is a general relationship between friction and wear change in the formulation that decreased wear tends to decrease friction. Wear could be reduced by using solid lubricants but it also reduces the friction. Wear is a slow process and is based on service life and not on any measurements of varying operating conditions and environment. Service life is not easy to determine, because in brake usage on different routes it results in different operating temperatures.

Figures of volume of friction material worn out per unit of energy dissipated can vary from 200 to 800 mm<sup>3</sup>/MJ.

### 1.15.3 Thermal Damage

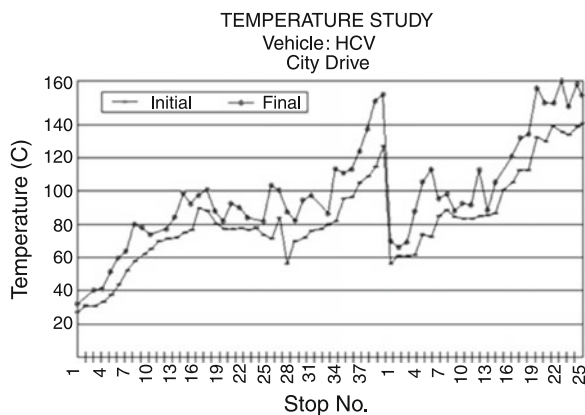
Designer of formulation should take note of localized heating and must ensure uniform distribution of heat over working area of the BFMC while giving serious process considerations. The material should have low modulus and be conformable to the opposing surface. Less the cross linking of the polymer, more thermally stable, will have lower modulus and especially during high-speed stops. Selection and nature, and proportion of usage of reinforcing fiber along with the polymer have a greater bearing on wear [101]. Titanium and vanadium in the cast iron disk can have a significant effect on friction and wear of the contacting surface disk. 0.03 % of titanium can halve the wear sometimes and is present in iron as very hard titanium carbon nitride particles [91].

## 1.16 Virtues of a Good Friction Material

Key characteristics in a brake friction material formulation—considerations while designing

- Adequate friction level to satisfy performance requirements of specific brake application.
- Stable friction over a range of operating temperatures at which brake is required to operate [55].
- Good compressibility (Fig. 1.25).
- Acceptable speed spread.
- Good fade/recovery characteristics.
- Adequate rate of wear throughout the operating temperature range.
- Compatibility with the contacting surface.
- High cold friction rating or no early morning sharpness.
- Minimum brake dust (mainly the black dust) and noise.

**Fig. 1.25** Temperature gradient in a HCV—city drive application



- Minimum fade with short stopping distance.
- Consistent performance across the range of temperature.
- No Noise-squeal, groan, Gu, Go and other noise levels.
- Low rotor wear.
- No judder due to adequate level of compressibility both hot and cold.
- Less disk thickness variation.
- No disk scoring issues.
- Adequate mechanical strength to withstand severity in service.
- Quick water recovery characteristics.
- Good bonding property.

In Fig. 1.25 trend of the temperature gradient graph in a heavy commercial truck or a bus chassis in a city drive route conditions indicates more frequent stops at slow speeds and pressures. The temperature increase has a sharp bearing on the noise and other performance-related issues normally addressed in the friction material design.

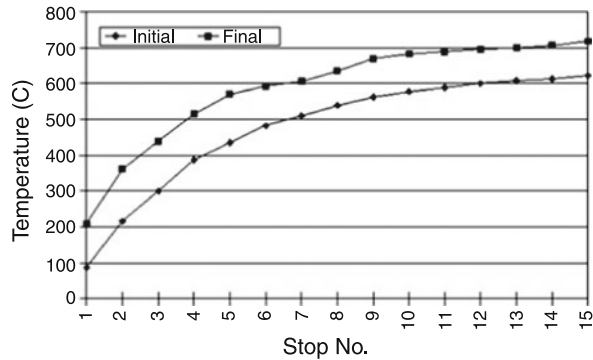
### 1.17 Key Characteristics of Friction Material Composite in Meeting the Above Said Virtues

- Modulus measurement to estimate toughness.
- Design hardness requirements of a system. An ideal mixture would exhibit hardness in the range 70–100 in the product and still have the required toughness.
- Mechanical strength to withstand the rigors of braking in question.
- Measure of critical stress intensity factor and energy factor  $K_c$  and  $K_e$ .
- Interference of modulus relative to each other. Modulus to be kept constant for a given range of measurement of other values of mechanical measurements. This is a key factor and should be validated for every change made in the design of formulation process.
- Higher deformation strength with resiliency in braking would be a good attribute at the contact and the contacting surface.  
Higher toughness reflects lower modulus in compression tension, and flexural bending strain. Toughness in the design could be achieved through matrix alteration as one bright option. Material design specification of the matrix (sequence given) below would give strong guidelines for improving the toughness.

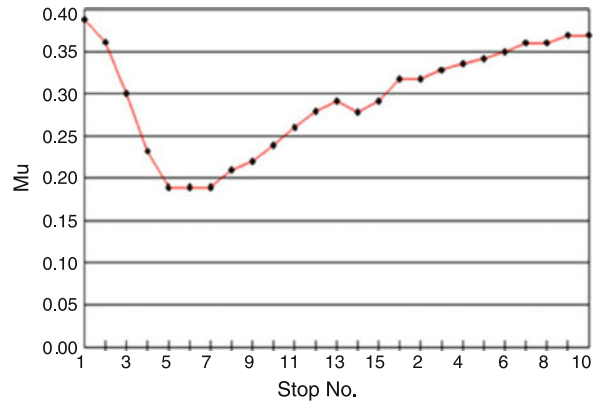
In Figs. 1.26 and 1.27, fading friction tested for a continuous repeat braking for 15 stops, temperature graph as high as 600–700 °C, initial increase of 350 °C with first 3 or 4 stops are a feature observed normally. This condition of the brake is envisaged in a downhill braking when the temperature peaks beyond 600 °C and fading friction become very significant.

Figure 1.27 shows  $\mu$  drops as low as 0.18–0.20 $\mu$  from 0.40 $\mu$  in the 5th–7th stop which is unacceptable in any class of brake pads. A minimum–minimum 0.22 $\mu$  is the design requirement on a scale of 0.42 $\mu$  and it is difficult to achieve such values in NAO pads and is possible to achieve in semimetallic and low metallic pads.

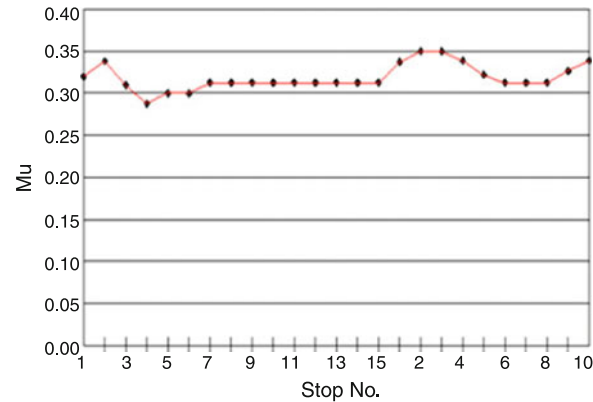
**Fig. 1.26** Disk pad temperature profile during fade test



**Fig. 1.27** Coefficient of friction showing fading and recovering friction levels



**Fig. 1.28** Fade, recovery graph



Further in Fig. 1.28 after the 15th stop when the fading friction averaged to 0.32–0.33 $\mu$  from 100 kmph speed to 0 kmph to a complete halt good recovery trend is observed. Drop in friction with the increasing speed in fade test on repeat stops with continuous braking is a definite trend. More depends on recovery trend and in

how many stops. Rapid drop and slow recovery over many stops is not considered a virtue in a friction material design.

Effect of speed shown in Fig. 1.29, with the drop in friction level beyond 100 kmph from  $0.40\mu$  to  $0.32\mu$ , indicates speed effect on braking. Similarly, temperature effect beyond 200–300 °C is given in the graph with the sharp drop in friction coefficient (Fig. 1.30).

Temperature, speed effect on  $\mu$  improves in the design by high temperature heat resistant friction modifiers like zirflor and stabilizing the friction with lubes like molybdenum disulfide and synthetic graphite without affecting the wear. Figure 1.31 shows the distinct variation in the testing between the small sample testing machine and a dynamometer test results with a huge trend variation. It is always preferred to do a dynamometer test than to be contented with SSTM (Fig. 1.32). Both are controlled simulated test machines, however, larger variation in friction levels are observed in SSTM results and misleads and misrepresents when compared with test data from a dynamometer. The wet friction test in Fig. 1.33 shows the characteristics in a friction material composite with very low friction in the first few stops to a good stable friction with further stops.

**Fig. 1.29**  $\mu$  profile with respect to speed

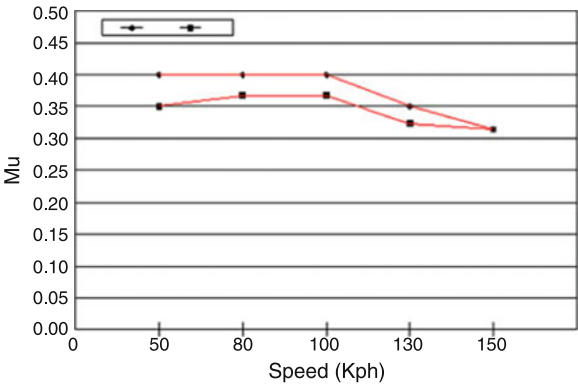


**Fig. 1.30**  $\mu$  profile with respect to temperature

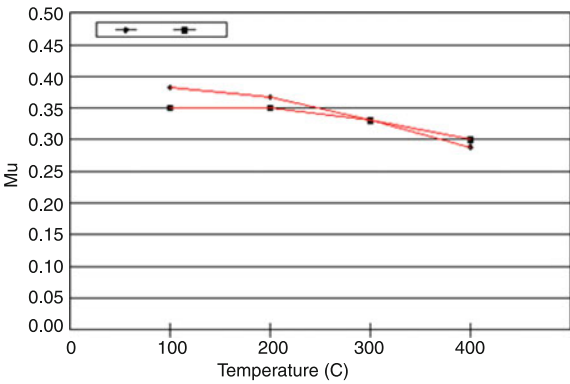


**Fig. 1.31** Comparison of fade versus recovery in a small sample testing machine and inertia dynamometer

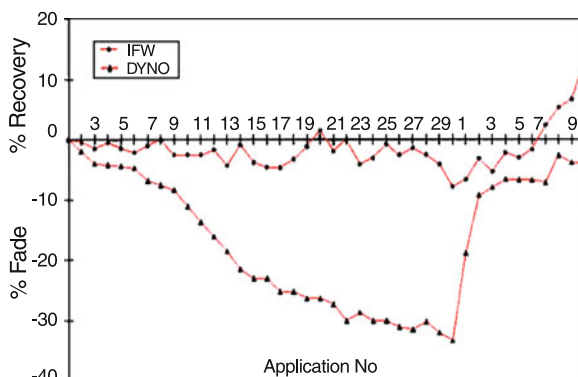
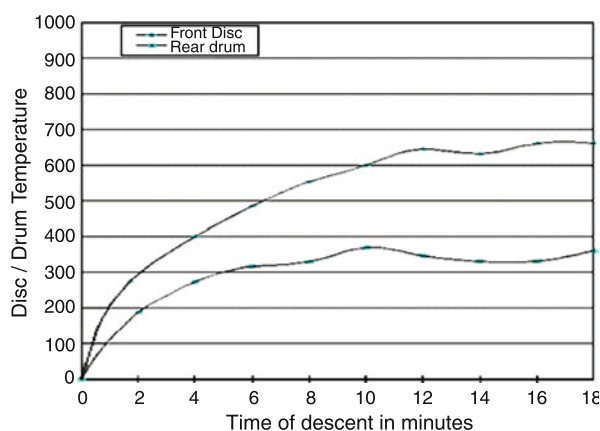


**Fig. 1.32** Typical temperature profile during hill descent test



## 1.18 Fading Friction

Fading friction for any given speed during uphill and downhill ride with continuous braking is more critical and essentially should never fade beyond 25 % as a braking safety criteria at temperatures as high as 600–700 °C. On the plains at high speeds with repeated applications fade should not drop as low as  $0.22\mu$ . Minimum–minimum  $\mu$  of 0.22 from the original level of  $0.41\text{--}0.43\mu$  in a high temperature stop is the lowest minimum acceptable to ensure brake safety. In a cold terrain at high speeds it is essential to meet the minimum fade which is difficult to achieve in a NAO Non-asbestos organic pad (normally met in semimetallic formulations with much ease).

Here, even at temperatures of 500–550 °C at high speeds in a cold terrain with outside temperatures dropping down to subzero, temperature enhances with a temporary drop during the stop. The temperature keeps increasing steadily in a fading cycle with repeat stops whether it is a cold or a hot terrain. Outside temperatures have minimum influence on the fade cycle and the temperature coming on the brake, whatever the heat dissipation loss that occurs (refer the attached torque trace Fig. 1.34 on high speed braking).

**Fig. 1.33** Wet friction characteristics

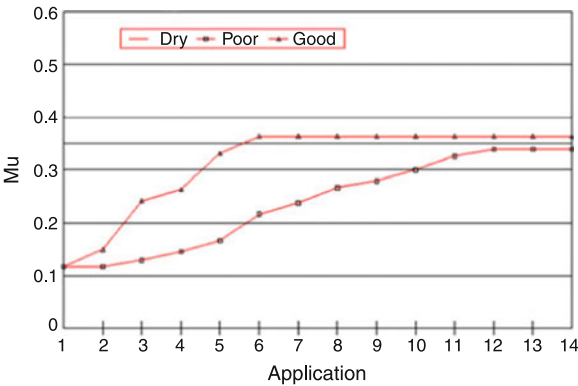
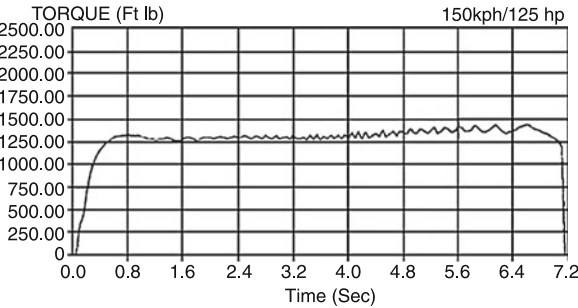


**Fig. 1.34** Torque trace of a high speed braking in a LCV model



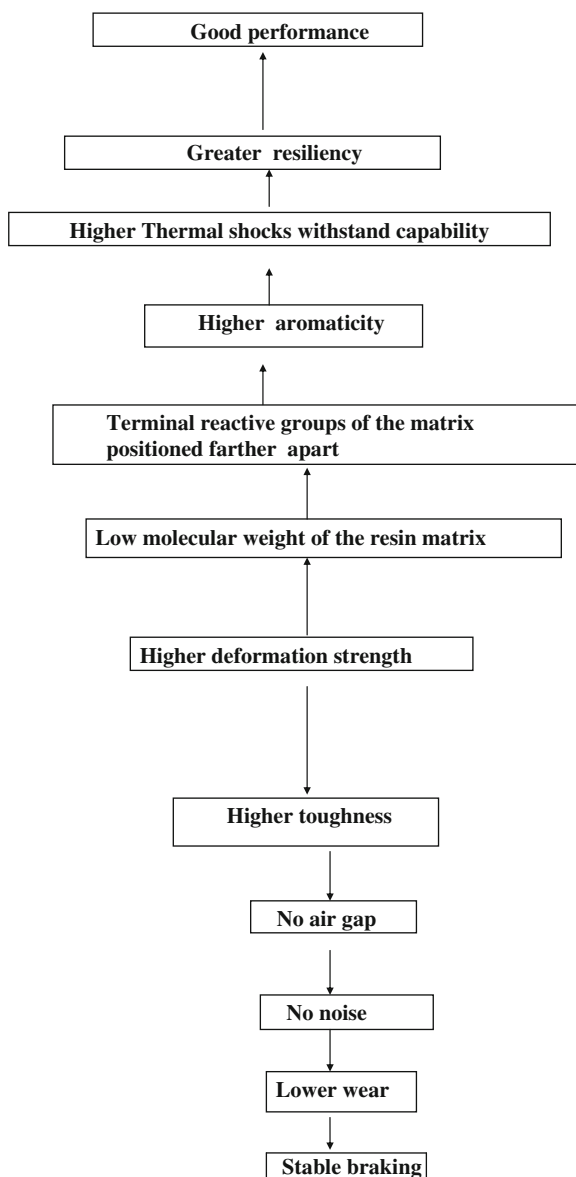
1.19 Noise Elimination Sequence

Braking noise is attributed to several different factors. Normally, in a high  $\mu$  performing pad/liner the noise is audible at higher temperatures on braking. There are several types of noise with varying frequencies at different operating conditions of cars, LCVs, and trucks. By and large, noise is directly related to BFMC design of materials besides the contacting conditions. It is an interesting science when we try to improve the toughness, we achieve higher deformation strength which can eventually eliminate noise. Toughness is an important characteristic in a friction material design which governs noise, braking performance, and wear.

For noise removal other than the usage of right shim, providing a chamfer, one should follow the sequence and go for  $\mu$ -V test as one option under the conditions stipulated below after making the necessary formulation changes. Matrix alteration with specification improvements to suit to the process directly relates to noise improvement as is given in the sequence below. Other than that, allow the pad to have a fan chamfer as is normally provided in pads. Combination of chamfer, suitable shims, and control on toughness in the design are warranted in some cases.

Brake pads have to be tested for static to dynamic  $\mu$  with 20 stops and look for maximum–minimum  $\mu$  and % drop in ratio normally indicates the level of noise reduction. Static to dynamic  $\mu$  ratio of 0 % will indicate no noise. It is achievable through matrix alteration and toughness improvement.

### ***1.19.1 Sequence to Control Good Braking, Low Wear with Minimal or No Noise***



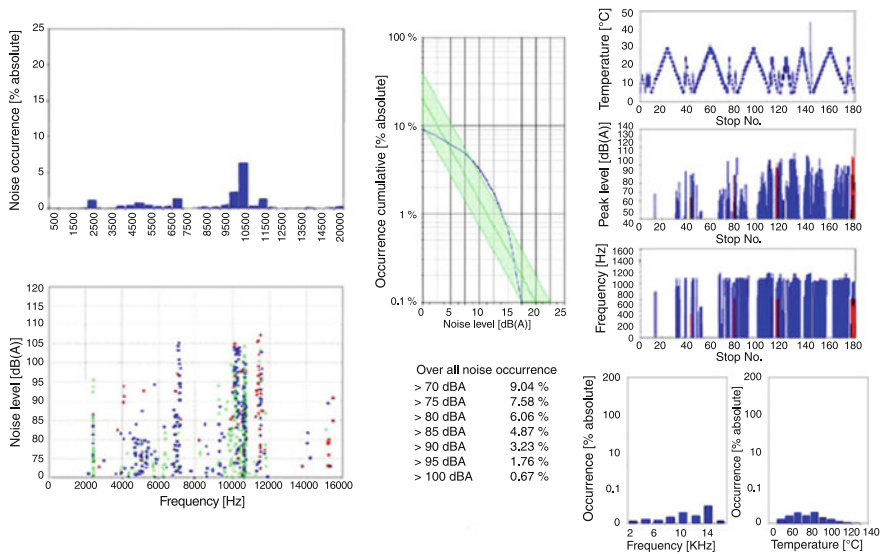


**Fig. 1.35** Noise occurrence in a brake pad sample—more pronounced at 11.5 kHz at low pressure and low temperature

Noise in a friction material brake pad or a liner is quite complex. Thorough understanding of the noise issue calls for extensive research and development in order to reduce and eliminate. Under noise classifications, there are different types of noises like groan, squeal, Gu, Go, as per various standards of classification. Noise in a drum brake, noise in a disk brake pad all have a general rule of varying frequency due to temperature, pressure, and sensitivity of certain raw materials in the system. Noise in friction material could be reasonably addressed through matrix alteration by elimination of air gap between the contacting surfaces during braking. It is possible to achieve higher deformation strength, higher toughness to get better resiliency in braking which eliminates noise. The above said sequence is achievable through matrix specification control like low molecular weight, lower impurities of free phenol content, flow control characteristics in the process.

In Fig. 1.35 specific high frequency noise at 11.5 kHz, more pronounced at 30 km speed in city road operation results from lower output, i.e., 30 bar pressure. Such specific issues could be addressed by providing Champer as a geometrical alteration with a fan type and an angle to be decided depending on the permissible wear limit for contact in a pad contact area [22, 25, 28] (Fig. 1.36).

Brake squeal phenomena is due to self-exciting vibration caused by fluctuation in the frictional force between the pad and the rotor (contact and contacting surfaces).

When the natural frequency of the system is a conjugate complex number, the vibrational system which is composed of caliper, pads, and rotor becomes dynamically unstable.

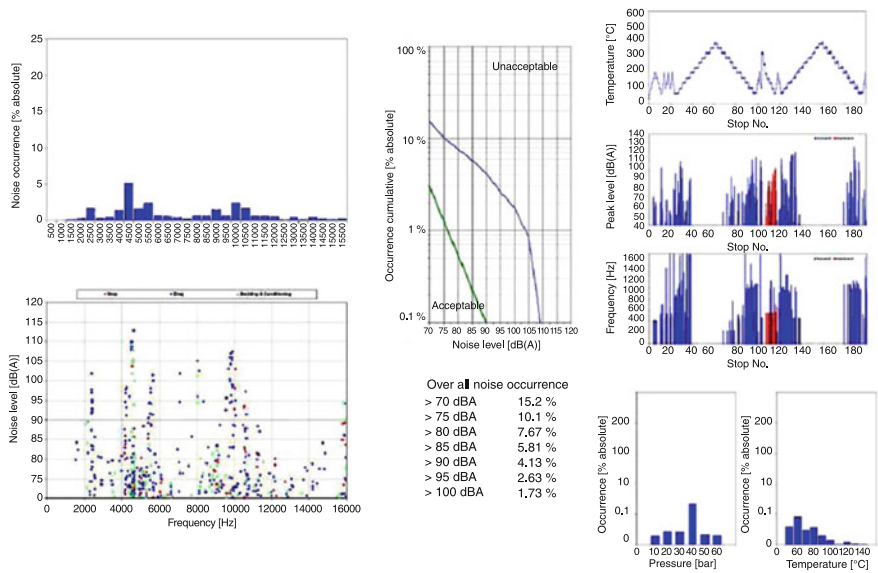


Fig. 1.36 Noise occurrence in a brake pad more pronounced in a range of frequencies

Brake squeal is normally above 5 kHz and shims are designed to annul the vibrational effect at higher frequencies. One needs to understand the brake component frequency response during braking with stabilized friction conditions. This can obviate the low frequency brake squeal while enabling to find the optimal rotor natural frequency. One can devise a method for measuring brake component frequency response during braking by oscillating the caliper, with friction surface condition stabilized. By doing so one can identify vibrational mode of brake component that can influence the squeal and the change in transient vibration characteristic before the squeal gets actually generated [23]. A theoretical kinetic energy model to know the factors that can influence brake squeal and the reduction process could be simulated [27].

Varying factors of braking force acting on a frictional contact surface of a pad/liner could be attributed to pad/liner contact versus (a) piston diameter, (b) thickness of the rotor, and (c) outer diameter of the rotor. Caliper is the receiver of the braking force which is connected to the steering knuckle.

Normally, brake squeals vary from 1.5 to 1.9 kHz, depending on the hydraulic pressure above 1 MPa no squeal gets generated normally. One can generate a frequency band for a given hydraulic pressure variation which normally ranges from 0.5 to 1 MPa. A laser Doppler Vibrometer can accurately measure diametral nodes with several points caused due to constant frequency vibration.

### ***1.19.2 The Vibration Components from the Radial Direction of the Rotor Has the Following Components***

Component in vertical direction to the rotor friction surface is normally seen in

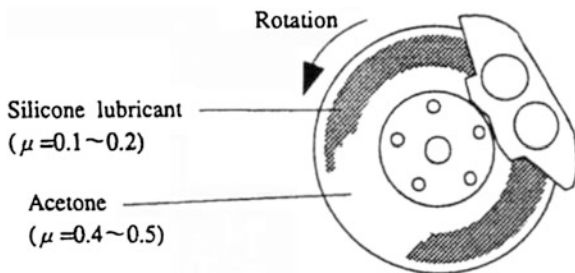
1. Rigid body.
2. Around the axis of the rotational component in radial direction to the rotor.
3. Diagonal elastic deformation component.

Vibration characteristic measurement could be measured with piezoelectric accelerometers to understand the squeal generation. For a given speed of the rotor and varying hydraulic pressures applied with oscillating waves to the caliper through electromagnetic shaker at any given point to the normal direction of braking surface rotor rotating direction. The coherence of acceleration/vibration load could be measured at each point. Normally coherence less than 1 MPa between the coefficient of friction of the material is not achievable in view of elastic properties, toughness, with fluctuation in pressure applying position. The toughness linear measurements depends more on the contact area of the friction material portion. A toughened material can measure each pressure application central to the piston center with varying dimensions to vary the toughness for a fixed pressure, say 0.8 MPa.

In Fig. 1.37 squeal generation characteristic could also be controlled by applying a lube to the rotor surface and measured by the varying friction coefficient [52, 53]. One would see a conspicuous drop in friction when the lube is applied and under such conditions it will not squeal. When the lube applied is thoroughly removed and tested we will see a conspicuous increase in friction from  $0.20\mu$  to  $0.45\mu$  when it will squeal. As  $\mu$  increases frequency response peak will appear which could be measured as a variation of frequency response in relation to friction coefficient.

Frequency response to be measured with vibration applied in the direction vertical to the rotor frictional surface. The peak generated at squeal generating frequency will increase as the friction coefficient  $\mu$  increases. In another case, frequency response measured in the rotor rotating direction will not show any peak in the squeal generating frequency band. Peaks may grow as and when the  $\mu$  increases. The reason for generation of brake squeal in the direction vertical to the

**Fig. 1.37** Squeal generation after applying lube—drop in friction coefficient



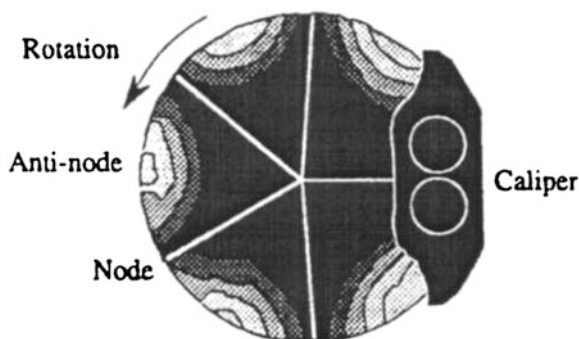


Fig. 1.38 Rotor friction surface coupled with rotor rotating direction

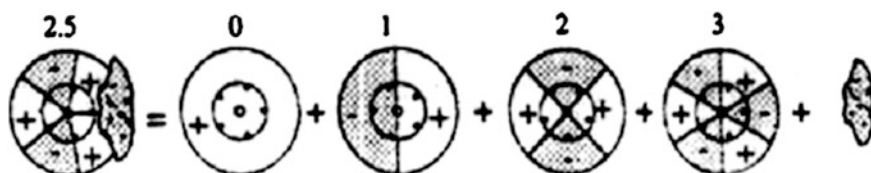


Fig. 1.39 Node

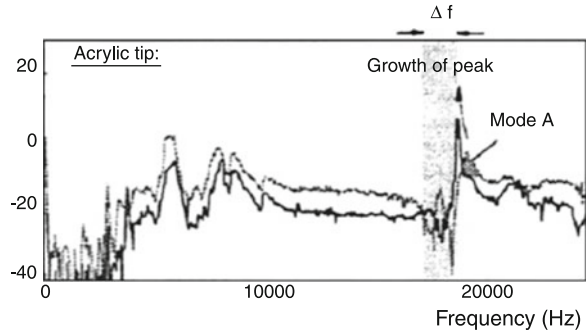
rotor friction surface is due to the fact it gets coupled with that of the rotor rotating direction.

As seen in the graphs (Figs. 1.37, 1.38, 1.39 and 1.40) the rotor cannot have 2.5 nodes in elastic vibration due to the fact that it is a result of 0–1 node vibrations, which is the vibration of the rigid body and 2- and 3-node vibration which is a flexible vibration. 3-node vibration with a natural frequency of 2 Hz contributes most to 2.5-node vibration. When a natural frequency is applied to the caliper in the rotor rotating direction the caliper undergoes diagonal elastic deformation. It goes to clearly explain the fact that the rotor is rigid and diagonal deformation [54] results in the generation of the squeal [33, 35]. Besides the larger influence of friction coefficient of material  $\mu$ , friction material linear toughness has greater bearing on the squeal generated.

In the case of low frequency brake squeal, it is a dynamically unstable [26, 29] phenomena and difficult to address as it is caused due to kinetic energy which influences the vibration system when pressure fluctuation between rotor and pads is combined with relative displacement in the direction vertical to the friction surface.

Series of noise peaks with range [30, 32] of frequencies are seen in Fig. 1.37. which could normally be addressed in the formulation material design with more controls on the matrix specifications. It demands formulation change and will need entire design change, with other issues under consideration which needs to be addressed while altering the design. It is always suggestible to go for a complete testing and validation for performance while making changes in the formulation for improving noise matrix

**Fig. 1.40** Diagonal deformation leading to squeal



at every stage. Modifying for noise can hamper other characteristics hence require validation at every step. In some cases, DOE with one or two limiting variables, i.e., matrix input ratio with specification changes are a good possibility. It could be tried in a partial fractional factorial design in order to minimize the number of tests. The above said noise sequence might help circumvent the extensive development effort by design alteration with validation at every stage for all the properties.

It could be tried in a partial fractional factorial design in order to minimize the number of tests. The above said noise sequence might help circumvent the extensive development effort by design alteration with validation at every stage for all the properties.

### ***1.19.3 Noise Search Graph***

See Fig. 1.41.

### ***1.19.4 Noise Occurrence with Pressure and Temperature***

See Figs. 1.42 and 1.43.

### ***1.19.5 Frequency Versus Peak Level Decibels in Relation to Temperature Scale***

See Fig. 1.44.

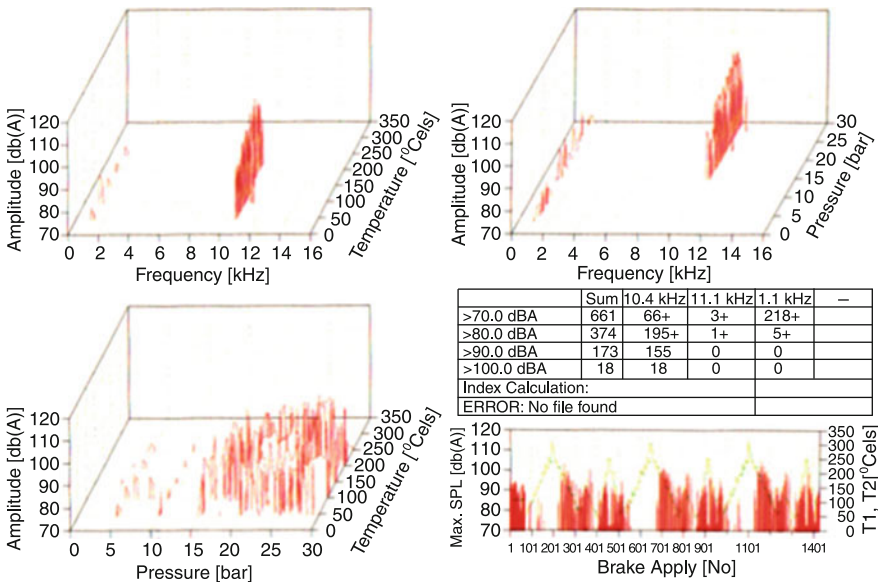


**Fig. 1.41** Noise search graph on applications—authors own disk pad sample tested in passenger car model

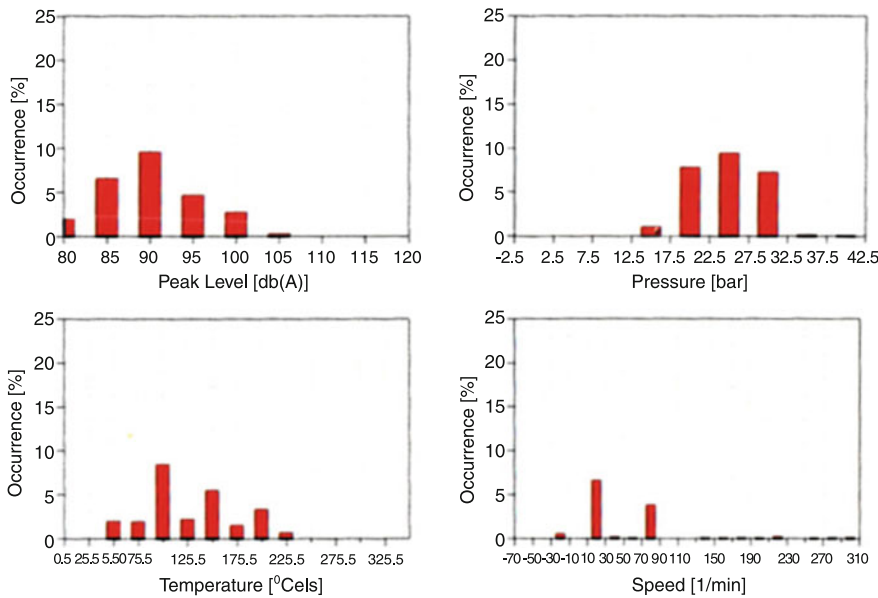


**Fig. 1.42** Noise occurrence with pressure, temperature, and speed variations

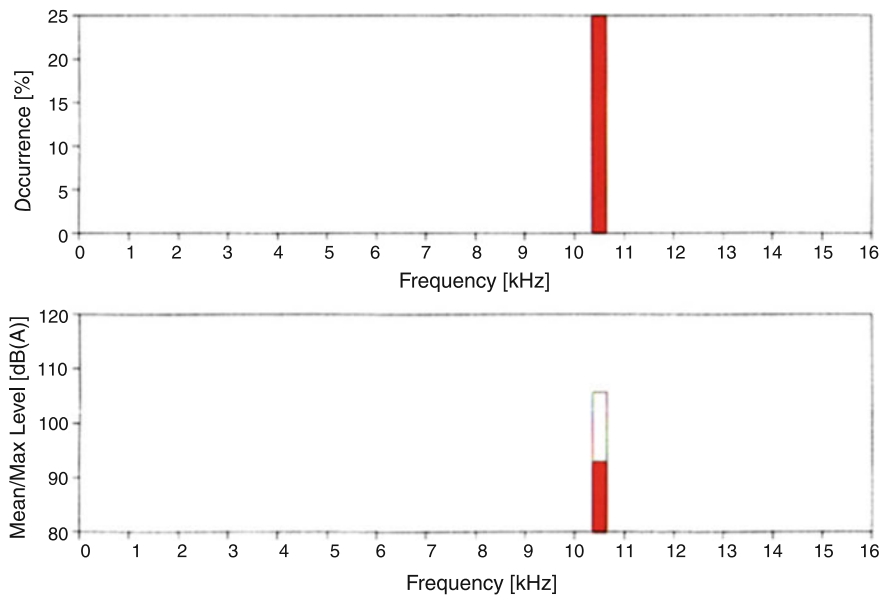


**Fig. 1.43** Typical noise search graph—authors own disk pad sample tested in passenger car model

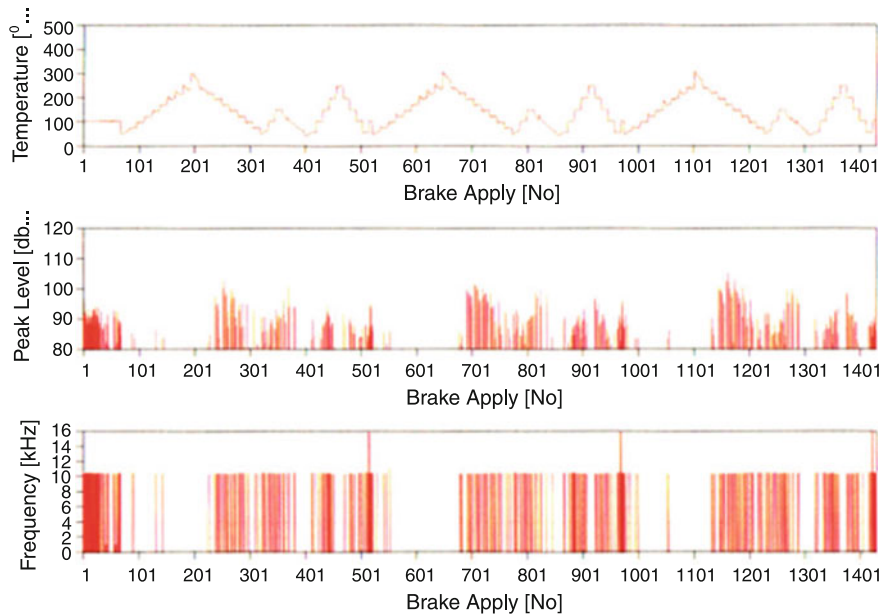


**Fig. 1.44** Frequency, peak level decibels, temperature scale over several applications. Noise search—authors own disk pad sample tested in passenger car model

1.19.6 Typical Noise Search for Varying Amplitude

An Account of Squeal Noise

The friction coefficient and the pad/disk stiffness, perpendicular to the friction force direction, are considered important parameters for disk brake squeal. This is based on theoretical considerations of the brake squeal excitation mechanisms and brake system modeling. However, this is without experimental verification on a real brake system (Fig. 1.45).

Because this work focuses on the disk/pad tribosystem parameter’s influence on brake squeal, the friction coefficient and the pad’s normal stiffness which will be under investigation. Experimental data using different brake pads the friction coefficient normally is proved to have the most single correlation to the brake squeal propensity, however, counterexamples to the general trend exist. In contrast to the friction coefficient, the pad’s normal stiffness is not in situ measurable with sufficient precision, so a model of the pad normal stiffness based on compressibility measurements could be used for modeling a clear trend of an increasing squeal propensity with increasing friction coefficient and increasing stiffness. There is always a local trend for the different friction material tests that are similar to global trend.

Linear squeal propensity regression models based on the friction coefficient and the stiffness could reveal the squeal propensity for each test. The deviations between the squeal propensity measurements and the calculated squeal propensities from the models are normally in a suitable range to reproduce general trends.

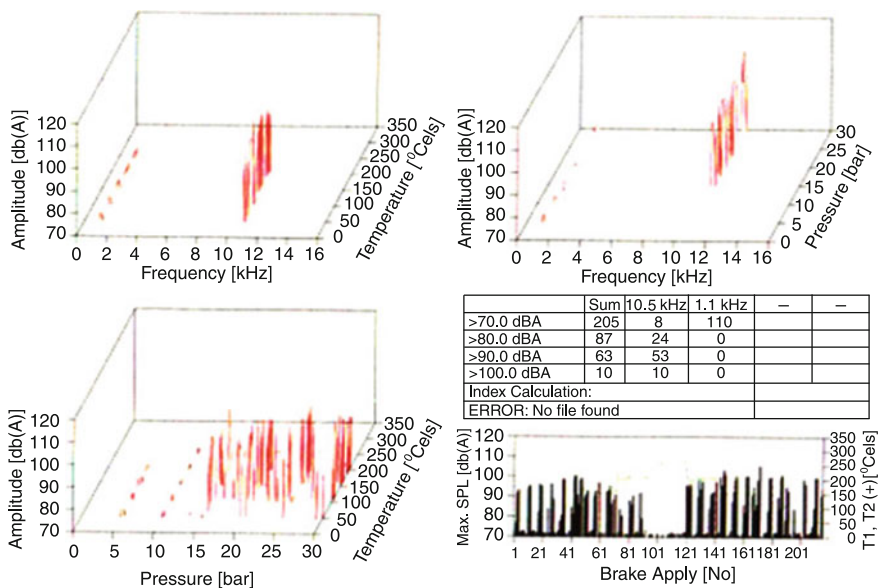


Fig. 1.45 Typical noise search for varying amplitude with decibels—authors own disk pad sample tested in passenger car model

However, the models cannot precisely estimate the squeal propensity. This might indicate the existence of additional (unconsidered) parameters.

Data mapping functions have been used to calculate characteristic values based on the friction coefficient and the pad normal stiffness, one per brake application or one per test.

The correlation between the squeal propensity and these characteristic values showed that the measured squeal propensity trends can be maintained throughout data pooling. By using specific characteristic values for squeal propensity models on the brake application and test timescale, the squeal propensity models are not worse than the measurement data based on squeal propensity models.

To judge the usefulness of the squeal behavior models, a ‘Model Quality Rating Measure’ helps in calculation of each test the squeal propensity regression model. The deviations between the calculated and the measured squeal propensities can help assess the model’s applicability. Additionally, the quality rating helps to arrange the different models by usefulness.

Squeal propensity models revealed a smallest deviation between measured and calculated squeal propensity for each test using a single characteristic value per test. It was based on the percentage of friction coefficient values above 0.5 during the test and on the modeled stiffness with a brake line pressure of 60 bar. This can support the assumption that higher friction coefficient values which drastically influence brake squeal and that the squeal propensity depends on the pad normal stiffness, perpendicular to the friction force direction (Figs. 1.46 and 1.47).

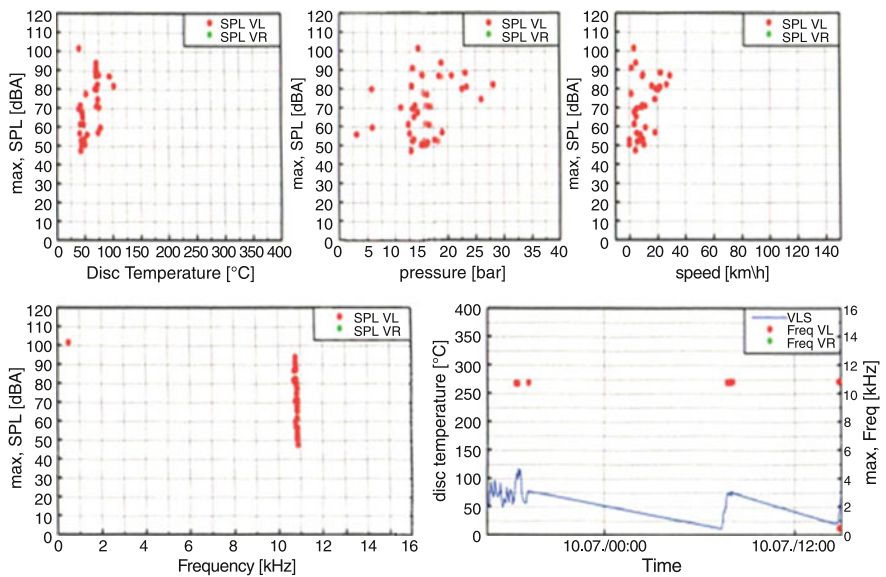


**Fig. 1.46** Noise search showing decibel variations—authors own disk pad sample tested in passenger car model

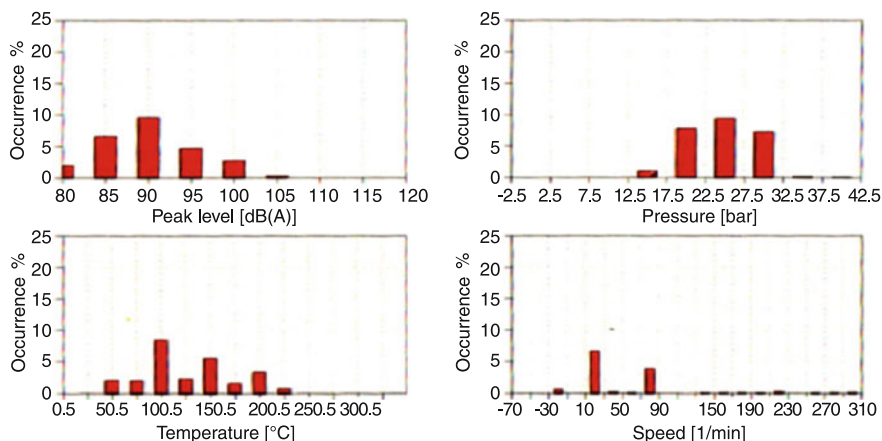


**Fig. 1.47** Noise occurrence with pressure, temperature, and speed variations—authors own disk pad sample tested in passenger car model

Source of this noise exhibited above is attributed to matrix polymer, which when brought under design specifications with control on friction stability and wear, gets eliminated as it is more pronounced in the higher frequency approximately 11.5 kHz, low pressure (30 bar), low temperature 100 °C, and in city road drive conditions.

## 1.20 Compressibility and Judder Vibration-Related Issues in a Disk Pad: Compressibility of the Pad—And Cold Hot

In Fig. 1.48, cold compressibility measured in a brakepad using BMI matrix (upper maximum average and lower maximum average (195–210  $\mu\text{m}$ ). At this level of compressibility of the pad, one can envisage the elimination of judder characteristics at high speeds with infrequent stops.

Similarly, in Fig. 1.49 is shown a marginal increase reaching the upper average limit of 210–215. In both the cases the pad material is a good compressible material and is less susceptible for judder characteristics [24] both at high and low speeds.

### 1.20.1 High and Low Speed Judder

Judder vibrations with frequencies are proportional to the turnover frequency of the wheel, consequently proportional to the speed of the car during braking. In most cases

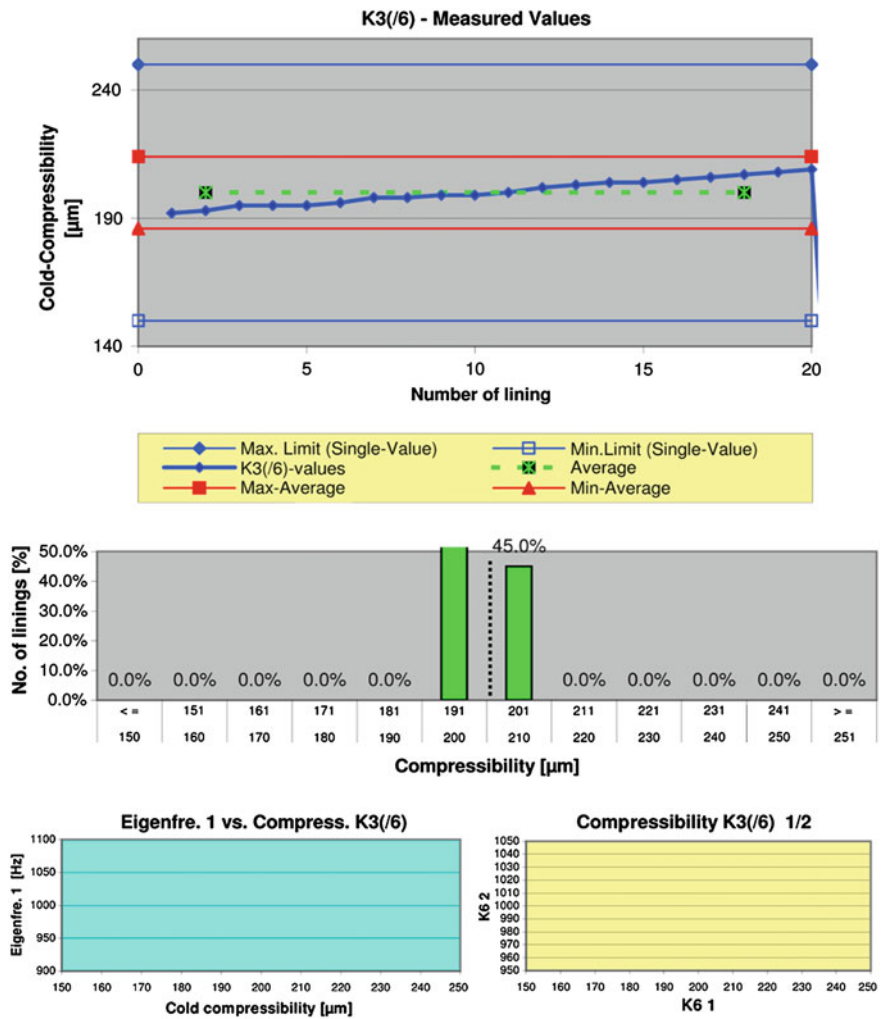


Fig. 1.48 Typical cold compressibility (authors own disk pad samples)

these vibrations have frequencies between 5 and 50 Hz. The lowest frequency is equal to the turnover frequency of the wheel and others being its harmonics [36, 37].

Origin of the judder is by the interaction between the surface of the brake disk and the friction material [92].

Steering wheel and the brake pedal are those elements of the car where the drivers feel the effect. Sometimes, acoustic judder or sound produced by vibrations of the body of the car is felt.

When perception judder vibrations occurs through the brake pedal, their origin is due to the variation of the pressure of brake liquid produced by the vibrations of the

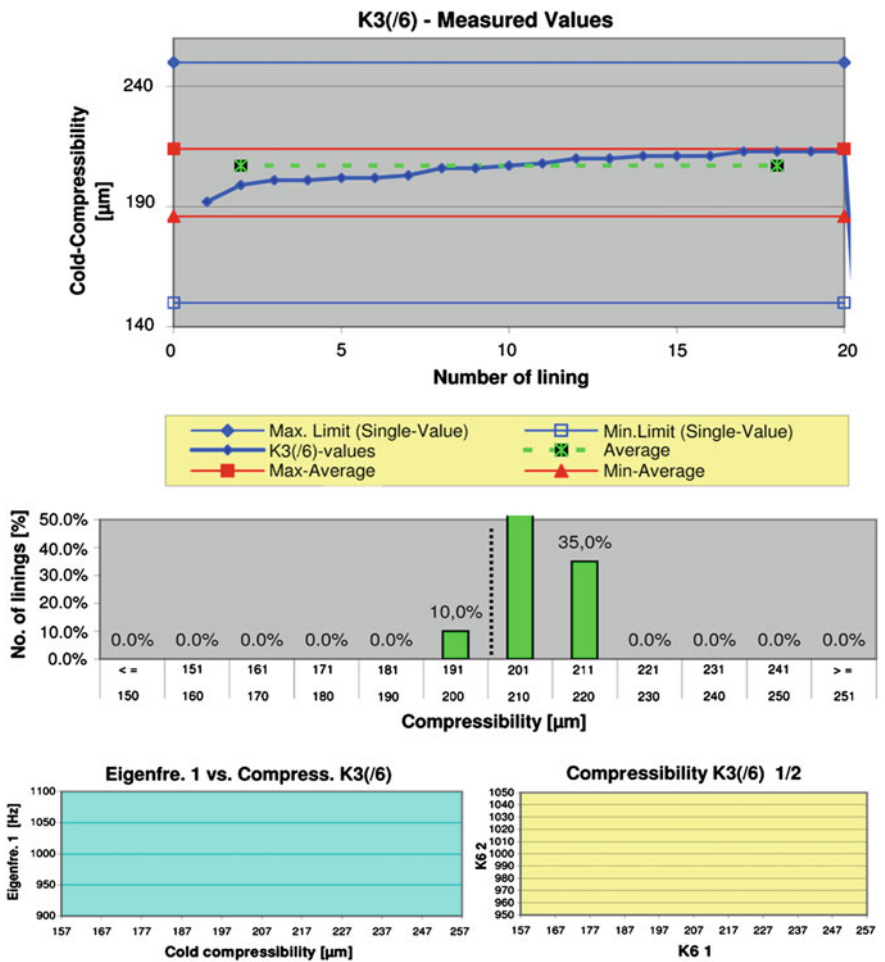


Fig. 1.49 Cold compressibility measured on another sample related to judder

piston of the caliper in contact with the brake pad assembly. Consequently, this type of vibration may be described as periodic displacement of the brakepad in the direction normal to the disk surface. The amplitude of the brake pressure variation (BPV) is the measure of the effect. Two principal mechanisms of BPV may be considered. First, is due to the mechanical defect known as “runout” of the brake disk during assembling. The second mechanism is due to the nonuniform wear of the disk surface.

The vibrations of the steering wheel during braking are associated with the displacement of the caliper in the direction tangential to the disk surface. The BTV and BPV phenomena are coupled because the friction force is proportional to the normal pressure. The relation between the amplitudes of the BTV and BPV depends on the parameters of the car. In some specific cases, strong BTV can be observed

without significant BPV because friction coefficient is not uniform over the disk working surface and thus BTV is sensitive to the composition and structure of friction interface.

It often happens that strong judder is observed after the brake disk has been heated up over 500 °C (fading). Such a treatment leads to the formation of a deposit of friction material on the disk surface [90] or so called “hot spots”. These deposits modify friction coefficient and thus cause BTV. At the same time, BTV can be observed when the thickness of such deposit becomes high (above 10  $\mu\text{m}$ ). This specific vibration is called “hot judder” indicating that it is produced after a heat treatment of the disk surface in contact with the friction material.

It may be improved by an assessment of the friction interface at lower temperatures when deposits are removed from the surface. In most applications, judder progressively increases with the wear of the disk. It happens that two surfaces of the disk are not perfectly planar and parallel due to the nonuniform wear. This is expressed as disk thickness variation over the working surface.

The empirical rule shows that disks with DTV above 20  $\mu\text{m}$  exhibit noticeable vibrations (BPV and BTV).

Problems related to disk composition, performance of the caliper, and properties of the friction material could contribute to DTV issues. It has been noticed that wear resistance of gray cast iron strongly differs with its composition and structure. Disk with higher hardness shows less DTV generation. Normally, floating calipers show better performance than the fixed ones. Composition and physical properties of friction material are of prime importance for the problem which is the essential part of the “knowhow” principle. Matrix alteration with specification variation while addressing the above said issues of judder could be done using materials like BMI with the right dosages. It also addresses the issues of rotor wear, hence good for judder.

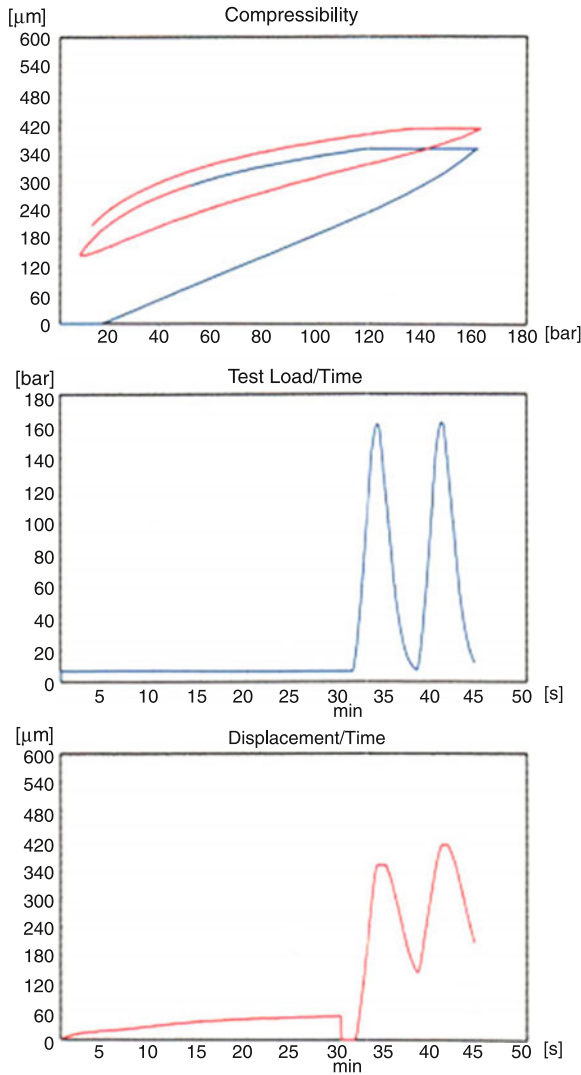
Low speed judder—due to long duration braking after running the vehicle for 20–30 min at 100–110 kmph, can cause faceout of the disk and disk thickness variation (DTV).

Low, high speed judder is related to compressibility of the pad (Fig. 1.50), which can lead to performance variation and is purely system dependent (Fig. 1.51) [38, 41].

First and last cycle load versus compression comparison—compression rate in two samples of the sample brake pad.

Similarly, high speed judder causes thermal deformation, distortion due to high energy inputs at high speeds 150–200 kmph to 0 kmph while one tries to bring the vehicle to a complete halt. Rotor distortions happen at high temperatures 500–600 °C causing disk thickness variation at high speeds when one stops. These issues get addressed in the design by controlling the hot and cold compressibility values brought under the specified limit.

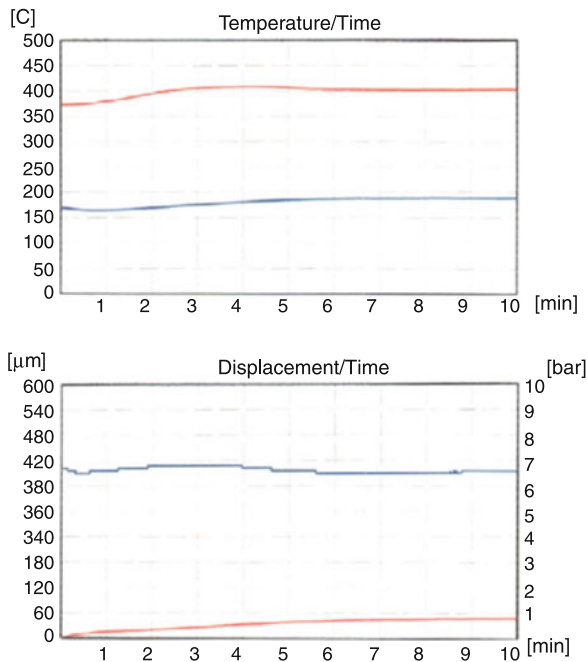
**Fig. 1.50** Load, displacement, temperature for range of time, versus compressibility in  $\mu\text{m}$  measured on a disk pad sample 1



**1.21 Kinetic Coefficient of Friction: Theoretical Considerations**

The kinetic coefficient of friction  $\mu$  is the ratio between the forces that oppose two materials ( $F_f$ ) and the force ( $N$ ) that holds them against each other when they are in motion.

**Fig. 1.51** Load, displacement, temperature for range of time, versus compressibility in  $\mu\text{m}$  measured on a disk pad sample II



$$\mu = \frac{F_t}{N}$$

Consider the case of a body that rests on a rough table as shown in Fig. 1.51. Its weight  $mg$  is acting downwards and normal reaction  $R$  is acting in the opposite direction such that the two balance each other (Figs. 1.52 and 1.53).

Now suppose we pull the body by a horizontal force  $P$ , then there will be a force of friction  $F$  in the opposite direction that prevents the motion of the body. Let the resultant  $R$  and  $F$  is  $S$  which makes an angle  $\theta$  with  $R$ . Resolving  $S$  along  $R$  and  $F$ , we have

$$S \cos \theta = R \quad \text{and} \quad S \sin \theta = F$$

$$\tan \theta = F/R$$

For the sake of equilibrium

$$R = W \quad \text{and} \quad F = P$$

If we keep increasing the pull, the force of friction keeps increasing till we arrive at a stage when the body is at the point of moving. This stage is called as limiting equilibrium. The force of friction in this case is called limiting friction (Fig. 1.54) and is maximum. The angle, which the resultant of this maximum force and normal

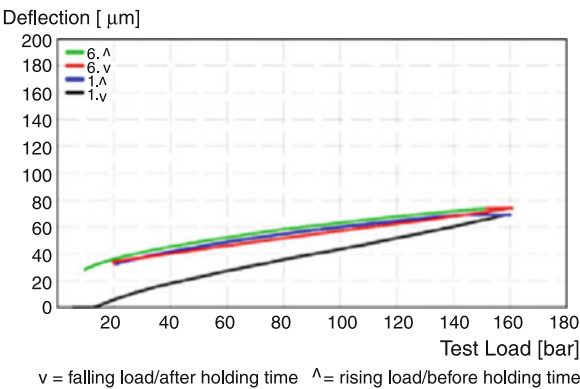


**Fig. 1.52** a Rising load before holding time, falling load after holding time—test load up to 180 bar versus deflections in  $\mu\text{m}$

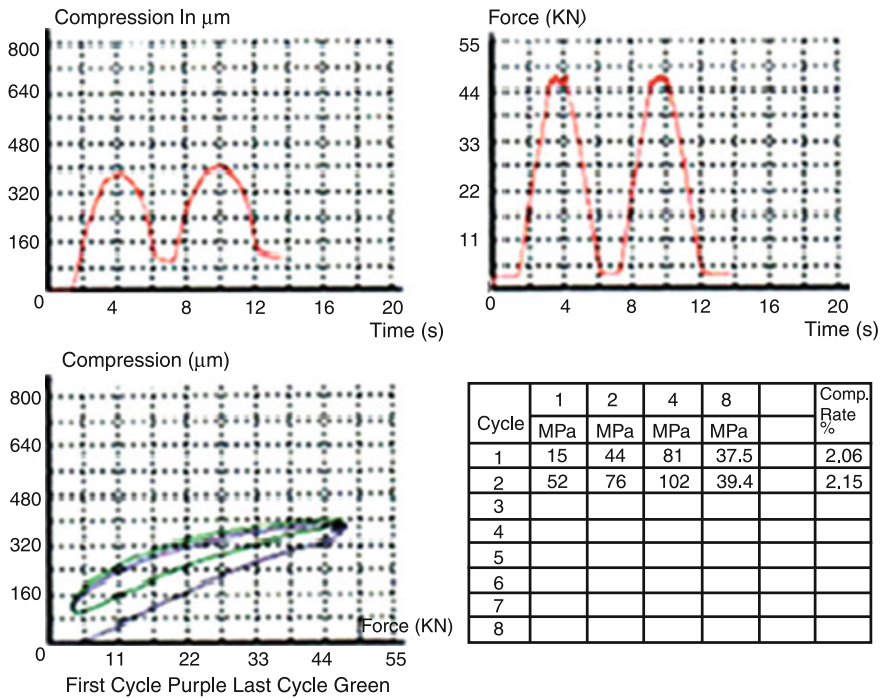
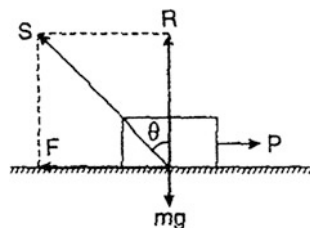


**Fig. 1.53** Load, displacement, temperature for range of time versus compressibility in  $\mu\text{m}$ -disk pad sample 2

**Fig. 1.54** Limiting friction, coefficient of friction and angle of friction



reaction makes with the normal, is called angle of friction. This is generally denoted by  $\mu$ .

The coefficient of friction  $\mu$  is the ratio of limiting friction  $F$  to the normal reaction  $R$  between two surfaces.

i.e.,

$$\mu = \frac{\text{limiting friction}}{\text{normal reaction}} = \frac{F}{R} \quad (1)$$

When the body is actually moving over the surface of another body, we replace  $F$  by  $F_k$ , and  $m$  by  $m_k$ . So,

$$\mu_k = F_k/R \quad (2)$$

the angle, whose resultant of limiting friction  $F$  and the normal reaction  $R$  makes with the normal is known as angle of friction and is denoted by  $\lambda$  (Fig. 1.55).

From Fig. 1.55,

$$\tan \lambda = F/R \quad (3)$$

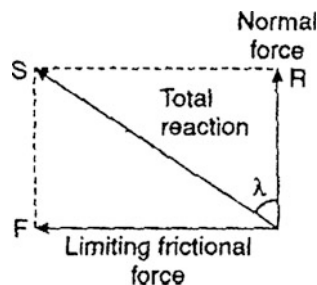
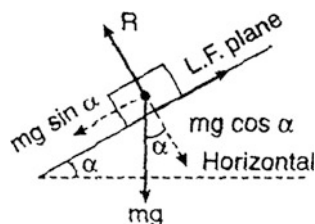
From (1) and (2), we have

$$\mu = \tan \lambda \quad (4)$$

The following points should be remembered:

- (1) Frictional force is independent of the velocity of body.
- (2) The coefficient of friction depends on, nature of the material, surface finish, surface film, and temperature.
- (3) During pulling a body, the normal component of the force decreases the weight of the body. Now the normal reaction decreases and hence the frictional force decreases. Because of which the pulling becomes easier.

**Angle of Repose ( $\alpha$ )** This angle is relevant to an inclined plane. If a body is placed on an inclined plane and is on the point of sliding down, then the angle of

**Fig. 1.55** Reaction between the two surfaces**Fig. 1.56** Angle of repose

inclination of the plane with the horizontal (Fig. 1.56) is called the angle of repose ( $\alpha$ ) for the two surfaces in contact.

$$F = mg \sin \alpha \text{ and } R = mg \cos \alpha$$

$$F/R = \tan \alpha = \mu \quad (1)$$

Again,

$$\mu = \tan \lambda \quad (2)$$

So,  $\alpha = \lambda$

Angle of repose = Angle of limiting friction.

**Laws of Friction** The following are the laws of friction:

- (1) The force of friction at the point of contact of two bodies is in the direction opposite to that in which the point of contact starts moving.
- (2) When the body is on the point of moving, the force of friction is limiting. The ratio of limiting friction to normal reaction bears a constant ratio and is denoted by  $\mu$ . The limiting friction is  $\mu R$ .
- (3) The limiting friction is independent of areas in contact provided the normal reaction is unaltered.
- (4) When the body starts moving, the above law of limiting friction still holds good and is independent of velocity.

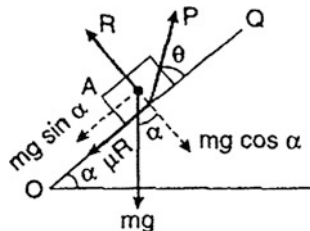
**Rolling Friction** When bodies such as wheels, spheres, cylinders rolls over a surface, the force of friction that comes into play, is called rolling friction. The rolling friction is denoted by  $(\mu_r)$ . It has been observed that the coefficient of rolling friction ( $\mu_r$ ) between two surfaces is much smaller than the coefficient of limiting friction ( $\mu$ ) for the same two surfaces. Due to this reason, it is easier to move a heavy load from one place to another by placing it over a cart with wheels than to slide it over the surface. So, wheels are used extensively in our daily lives for transportation.

We have studied that rolling friction becomes much smaller than the sliding friction. This is the principle on which ball bearings work. In ball bearing, hard steel balls are placed between the moving parts such as coaxial cylinders. The axle attached to the wheel fits tightly into the inner cylinder, while the wheel is put in firm contact with the outer cylinder. When the axle rotates (say in clockwise direction), the steel balls rotate in the opposite direction (in anticlockwise direction). So the outer cylinder rotates in anticlockwise direction. As the two cylinders have rolling motion relative to each other, the friction is considerably reduced to a large extent.

**Lubrication** When we put a lubricant (oil or grease) between the surfaces in contact, it is known as lubrication. The lubricant forms a thin layer between the two surfaces and hence avoids direct contact. In fact, by lubrication, dry friction is converted into fluid friction, which of course, is comparatively lesser in magnitude. In heavy machines, continuous supply of oil or some other suitable lubricant is provided to reduce the friction as well as to protect the moving part from overheating. Flow of compressed air is also used as lubricant. It reduces the friction between moving parts by acting as an elastic cushion and carries away the heat generated. It has the advantage of preventing dust and dirt from collecting over the moving part.

**Least Force Required to Pull a Body Up or Down a Rough Inclined Plane** Let a body  $A$  of mass  $m$  be placed on a rough surface  $OQ$  of inclination  $\alpha$ . The weight  $mg$  will be acting vertically downwards and the normal reaction  $R$  will be acting normal to  $OQ$ . Let an external force  $P$  be applied on the body at an angle  $\theta$ . Now, we shall consider the following two cases (Fig. 1.57):

**Fig. 1.57** Motion up the plane



*Motion up the plane*

When the body is just on the point of moving up the plane, the friction is limiting and the force of friction  $\mu R$  acts down the plane. Resolving along and perpendicular to the plane, we have

$$P \cos \theta = \mu R + mg \sin \alpha$$

or

$$\mu R = P \cos \theta - mg \sin \alpha \quad (1)$$

and

$$P \sin \theta + R = mg \cos \alpha$$

or

$$R = mg \cos \alpha - P \sin \theta \quad (2)$$

Substituting the value of  $R$  from (2) into (1), we get

$$\mu[mg \cos \alpha - P \sin \theta] = P \cos \theta - mg \sin \alpha$$

or

$$mg[\mu \cos \alpha + \sin \alpha] = P[\cos \theta + \mu \sin \theta]$$

or

$$mg[\tan \lambda \cos \alpha + \sin \alpha] = P[\cos \theta + \tan \lambda \sin \theta]$$

$$mg \left[ \frac{\sin \lambda \cos \alpha + \cos \lambda \sin \alpha}{\cos \lambda} \right] = P \left[ \frac{\cos \theta \cos \lambda + \sin \lambda \sin \theta}{\cos \lambda} \right]$$

or

$$mg \sin(\alpha + \lambda) = P \cos(\theta - \lambda)$$

$$\therefore P = \frac{mg \sin(\alpha + \lambda)}{\cos(\alpha - \lambda)} \quad (3)$$

The force  $P$  will be least when

$$\cos(\theta - \lambda) = 1 \text{ or } \theta - \lambda = 0$$

i.e.,  $\theta = \lambda$  then

$$(P)_{\min} = mg \sin(\acute{\alpha} + \lambda) \quad (4)$$

*Motion down the plane*

In this case,

$$\mu R = P \cos \theta + mg \sin \acute{\alpha} \quad (5)$$

and

$$R = mg \cos \acute{\alpha} - P \sin \theta \quad (6)$$

Now,

$$\mu[mg \cos \acute{\alpha} - P \sin \theta] = P \cos \theta + mg \sin \acute{\alpha}$$

Simplifying, we get

$$P = mg \sin(\lambda - \acute{\alpha}) / \cos(\theta - \lambda)$$

The force is least, when

$$\cos(\theta - \lambda) = 1 \text{ or } \theta = \lambda$$

Now,

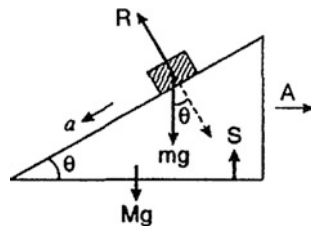
$$P_{\min} = mg \sin(\lambda - \acute{\alpha}) \quad (7)$$

*Fictitious force*

Common experience dictates that when a train accelerates or decelerates, a passenger in it experiences a force pushing him backward or forward respectively. Thus, even though there are no external forces acting on the passenger, he feels a backward or forward force as the case may be. The force is called fictitious force. The reason for this force is that the motion of the passenger is in an accelerated frame of reference. We can apply Newton's laws to a body in the accelerated frame of reference by considering that a force— $ma$  acts on the body, where  $m$  is the mass of the body and " $a$ " is the acceleration of the frame of reference. Due to the fictitious force, a passenger falls forward when a bus suddenly stops.

Similarly, when a train moves along a curved track, a passenger in it feels a force pushing him outwards away from the center of a curvature. The reason is that the

**Fig. 1.58** Inclined plane with an acceleration



motion of the train along a curved surface is an accelerated frame. Here the train is pulled inward by centripetal force and the passenger feels an outward centrifugal force.

Motion of a particle on smooth inclined plane is capable of horizontal motion on smooth table.

Consider a particle of mass  $m$  placed on the smooth face of an inclined plane of mass  $M$  and slope  $\theta$ , free to slide on smooth horizontal plane in a direction perpendicular to its edge.

As the particle moves down the face of an inclined plane, the inclined plane moves horizontally towards right with acceleration  $A$  (see Fig. 1.58).

Consider the vertical components of the forces acting on the particle. Applying Newton's second law, we have

$$mg - R \cos \theta = ma \sin \theta \quad (1)$$

For horizontal components, the motion of the particle is considered on acceleration frame of reference. So, a horizontal fictitious force acts opposite to  $A$ , i.e., there is a fictitious force  $mA$  to the left. Hence for horizontal component

$$R \sin \theta + mA = ma \cos \theta \quad \text{or} \quad R \sin \theta = m(a \cos \theta - A) \quad (2)$$

Now consider the forces on inclined plane. The forces are shown in Fig. 1.59. Here  $R$  and  $S$  are the third law forces.

In this case,

$$R \sin \theta = MA \quad (3)$$

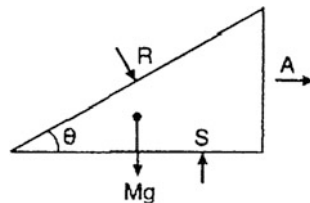
and

$$R \cos \theta + Mg = S \quad (4)$$

From (2) and (3), we get

$$m(a \cos \theta - A) = MA$$

**Fig. 1.59** Forces acting on an inclined plane



or

$$ma \cos \theta = A(M + m)$$

or

$$A = \frac{ma \cos \theta}{(M + m)} \quad (5)$$

From (3)

$$R = \frac{MA}{\sin \theta} = \frac{Mma \cos \theta}{(M + m) \sin \theta} \quad (6)$$

Substituting the values of  $R$  in (1), we get

$$mg - \frac{Mma \cos^2 \theta}{(M + m) \sin \theta} = ma \sin \theta$$

or

$$mg = ma \sin \theta + \frac{Mma \cos^2 \theta}{(M + m) \sin \theta}$$

$$a \left[ \sin \theta + \frac{M \cos^2 \theta}{(M + m) \sin \theta} \right] = g \quad (7)$$

If the particle starts from rest, the distance  $s$  moved in  $t$  second is given by

$$s = \frac{1}{2} at^2 \quad (8)$$

where  $a$  is its acceleration (given by (7)).

Friction Material Composites

Copper-/Metal-Free Material Design Perspective

Sundarkrishnaa, K.

2015, XXXIV, 372 p. 169 illus., 67 illus. in color.,

Hardcover

ISBN: 978-3-319-14068-1